arXiv:1502.06596v2 [hep-th] 18 Apr 2015

NORDITA-2015-24

Fractional Skyrmions and their molecules

Sven Bjarke Gudnason[1, 2, *] and Muneto Nitta[3, †]

[1]*Institute of Modern Physics, Chinese Academy of Sciences, Lanzhou 730000, China*
[2]*Nordita, KTH Royal Institute of Technology and Stockholm University,*
Roslagstullsbacken 23, SE-106 91 Stockholm, Sweden
[3]*Department of Physics, and Research and Education Center for Natural Sciences,*
Keio University, Hiyoshi 4-1-1, Yokohama, Kanagawa 223-8521, Japan

(Dated: April 21, 2015)

Abstract

We study a Skyrme-type model with a quadratic potential for a field with S^2 vacua. We consider two flavors of the model, the first is the Skyrme model and the second has a sixth-order derivative term instead of the Skyrme term; both with the added quadratic potential. The model contains molecules of half Skyrmions, each of them is a global (anti-)monopole with baryon number 1/2. We numerically construct solutions with baryon numbers one through six, and find stable solutions which look like beads on rings. We also construct a molecule with fractional Skyrmions having the baryon numbers $1/3 + 2/3$, by adding a linear potential term.

---

[*] Electronic address: bjarke(at)impcas.ac.cn

[†] Electronic address: nitta(at)phys-h.keio.ac.jp

I. INTRODUCTION

Half a century ago Skyrme made a proposal [1] that Skyrmions, i.e. topological objects characterized by the third homotopy group π_3, could describe nucleons in the pion effective field theory [2] if augmented by a higher-order derivative term. This term was then later denoted as the Skyrme term. The Skyrme term is needed for stabilizing the Skyrmions against shrinkage. Later nucleons are known to be bound states of quarks, described by QCD. However, QCD at low energies is strongly coupled and hard to tackle and hence the Skyrme model, with its small number of parameters, has remained an attractive model at low energies. In the limit of a large number of colors, the Skyrmion is exactly the baryon [3]. It has also recently been used in holographic QCD [4, 5].

It has recently been found that half Skyrmions stably appear as constituents of a lattice at finite baryon density [6]. It is therefore important to understand the physical consequences of a half or non-integer topological charge of half (or fractional) Skyrmions, such as the statistics of them. It is, however, not easy to pick up an isolated half Skyrmion because it is not stable in isolation.

The fractionality of topological charge, however, has been better understood in lower dimensions. As a lower-dimensional analog of Skyrmions, baby Skyrmions were proposed in an O(3) sigma model with a fourth-order derivative term in 2+1 dimensions [7, 8], which topologically are lumps characterized by π_2 instead of π_3, i.e. the case for usual Skyrmions. 2+1 dimensional Skyrmions often appear in various condensed-matter systems such as ferromagnets and quantum-Hall systems. A baby-Skyrme model with an XY-type potential $V = m^2 n_3^2$ (which is also called easy-plane in ferromagnets) admits half baby Skyrmions [9–11]. Each of them can be regarded as a global vortex covering the northern or southern hemisphere of the target space and consequently having a half π_2 topological charge. Each of them has logarithmically divergent energy when (if) isolated, because it is a global vortex. If one separates the two by an infinite distance, the energy diverges logarithmically and thus they are confined to the form of a molecule. If a U(1) subgroup of the O(3) symmetry in the O(3) model is gauged, each constituent baby Skyrmion becomes a local vortex (here the fourth-order derivative term is not needed for stability), (still) carrying half a unit of π_2 charge [12–15]. In this case, if we choose the gauge coupling and the scalar coupling to be the same, the baby Skyrmions are BPS and can be embedded in a supersymmetric theory

[14]. An entire molecule can be separated from other molecules without any cost of energy. In this phase the two half Skyrmions can be separated by a finite distance at a finite cost of energy. In this sense, the half Skyrmion can be isolated.

In this paper, we construct 3+1 dimensional half Skyrmions and their molecules in two Skyrme models with a potential term in the form of $V = m^2 n_4^2$, where we use the notation of the O(4) sigma model $n_A(x)$ ($A = 1, 2, 3, 4$) with the constraint $\sum_A (n_A)^2 = 1$. This potential is a potential for the would-be S^2 vacuum moduli and we will denote it a Heisenberg-type potential. The two models we consider in this paper are the conventional Skyrme model and a Skyrme-like model with the fourth-order derivative term replaced by a sixth-order derivative term. The latter is inspired by the BPS Skyrme model [16]. The sixth-order derivative term is the baryon-current density squared [16–19] and this term alone with an adequate potential provides the basis of an integrable subsector of the model. For a short-term notation, we call them the 2+4 and 2+6 model, respectively. Each constituent of the molecule is a half Skyrmion carrying half a baryon number, i.e. the topological charge of π_3. This turns out to be the case for both the 2+4 and the 2+6 models. The constituents are more separated for the 2+6 model than for the 2+4 model. This is in contrast with the conventional Skyrmions (i.e. without our potential) for which the configuration for $B = 1$ is spherically symmetric, that for $B = 2$ is toroidal, and those for $B > 2$ have energy distributions with some point symmetry [20, 21]. We take also the limit of the mass-parameters of our potential going to zero and recover the spherically symmetric Skyrmion for $B = 1$ and the transition is smooth as expected. We construct also higher baryon numbered solutions numerically; specifically $B = 2, 3, 4, 5, 6$ and find that the lowest-energy states are found using an axially symmetric initial guess (basically a torus) and the relaxation method finds the solutions which look like beads on rings. We confirm that the configurations of the form of beads on rings are really the lowest-energy states, by checking different initial conditions; i.e. both those with an axial symmetric Ansatz and others with a rational map Ansatz having an appropriate point symmetry [20, 21]. The rings of higher B are all stable against decaying into a sum of smaller B rings (for the B we have found explicitly here). This is a three-dimensional analog of baby Skyrmions as beads on a ring in a baby-Skyrme model with the XY-potential [10, 11]. We also construct fractional Skyrmions with an arbitrary baryon number by using the potential $V = m^2(n_4 - c)^2$, for which each unit Skyrmion charge is split into two fractional Skyrmions with baryon number $(1 + c)/2$ and $(1 - c)/2$, respectively. We call them unequal fractional molecules. We also note that fractional Skyrmions can be identified as global monopoles having divergent energy in an infinite system.

If one gauges an SO(3) subgroup acting on n_1, n_2, n_3 (a diagonal subgroup of the chiral symmetry), a monopole becomes the local 't Hooft-Polyakov monopole having finite energy [22–29], similarly to a vortex as a half lump in 2+1 dimensions [12, 14, 15]. Our case is a global analog of this case.

This paper is organized as follows. In Sec. II, we present our two models and their numerical solutions in Sec. III, i.e. of fractional-Skyrmion molecules. In Sec. IV, we construct an isolated fractional Skyrmion as a global monopole. In Sec. V, numerical solutions with higher baryon numbers $B = 2, 3, 4, 5, 6$ are presented. Finally, in Sec. VI, we construct a molecule where the weight of the two constituents of the molecule is altered, i.e. an unequal fractional molecule. Sec. VII is devoted to a summary and discussions. Two investigations are delegated to the appendices. In App. A we try different initial guesses for the numerical relaxation and find only metastable solutions. Finally, App. B shows how the molecule turns into a spherical Skyrmion by turning off the potential under study.

II. A SKYRME-LIKE MODEL WITH A HEISENBERG-TYPE POTENTIAL

We consider the SU(2) principal chiral model with the addition of the Skyrme term and a sixth-order derivative term in $d = 3 + 1$ dimensions. In terms of the SU(2)-valued field $U(x) \in \mathrm{SU}(2)$, the Lagrangian which we are considering is given by

$$\mathcal{L} = -\frac{c_2}{4}\mathrm{tr}\,(\partial_\mu U^\dagger \partial^\mu U) + c_4\mathcal{L}_4 + c_6\mathcal{L}_6 - V(U), \tag{1}$$

where we use the mostly-positive metric and the higher-derivative terms are given by

$$\mathcal{L}_4 = -\frac{1}{32}\mathrm{tr}\,(\left[U^\dagger\partial_\mu U, U^\dagger\partial_\nu U\right]^2), \tag{2}$$

$$\mathcal{L}_6 = \frac{1}{144}\left(\epsilon^{\mu\nu\rho\sigma}\mathrm{tr}\left[U^\dagger\partial_\nu U U^\dagger\partial_\rho U U^\dagger\partial_\sigma U\right]\right)^2, \tag{3}$$

where we are using Skyrme units in which lengths are measured in units of $2/(ef_\pi)$ and energy is measured in units of $f_\pi/(2e)$. $\mathcal{L}_4$ is the Skyrme term and $\mathcal{L}_6$ is the baryon current density squared, which is inspired by the BPS Skyrme model [16]. The symmetry of the Lagrangian for $V = 0$ is $\tilde{G} = \mathrm{SU}(2)_{\mathrm{L}}\times\mathrm{SU}(2)_{\mathrm{R}}$ acting on U as $U \to U' = g_{\mathrm{L}} U g_{\mathrm{R}}^\dagger$. In the vacuum, this symmetry is spontaneously broken down to $\tilde{H} \simeq \mathrm{SU}(2)_{\mathrm{L+R}}$, which in turn acts on U as $U \to U' = gUg^\dagger$, giving rise to the target space $\tilde{G}/\tilde{H} \simeq \mathrm{SU}(2)_{\mathrm{L-R}}$. The conventional potential term in the Skyrme model, viz. the pion mass term, is $V = m_\pi^2 \mathrm{tr}\,(2\mathbf{1}_2 - U - U^\dagger)$, and it *explicitly* breaks the symmetry $\tilde{G}$ to $\mathrm{SU}(2)_{\mathrm{L+R}}$.

In this paper, it will prove convenient to use the following notation of an O(4) nonlinear sigma model where we express the field U in terms of four real scalar fields $n_A(x)$ ($A = 1,2,3,4$) with the constraint $\sum_A n_A^2 = 1$:

$$U = in_a\sigma^a + n_4\mathbf{1}_2 \equiv \mathbf{n}\cdot\mathbf{t}\,, \tag{4}$$

where $a = 1,2,3$ is summed over, σ^a are the Pauli matrices and $U^\dagger U = \mathbf{1}_2$ is equivalent to $\mathbf{n}\cdot\mathbf{n} = 1$. We thus obtain the O(4) sigma model with the Skyrme and six-derivative terms

$$\mathcal{L} = -\frac{c_2}{2}\partial_\mu\mathbf{n}\cdot\partial^\mu\mathbf{n} + c_4\mathcal{L}_4 + c_6\mathcal{L}_6 - V(\mathbf{n}), \tag{5}$$

$$\mathcal{L}_4 = -\frac{1}{4}\left[(\partial_\mu\mathbf{n}\cdot\partial^\mu\mathbf{n})^2 - (\partial_\mu\mathbf{n}\cdot\partial_\nu\mathbf{n})^2\right]\,, \tag{6}$$

$$\begin{aligned}\mathcal{L}_6 &= \frac{1}{36}\left(\epsilon^{ABCD}\epsilon^{\mu\nu\rho\sigma}n_A\partial_\nu n_B\partial_\rho n_C\partial_\sigma n_D\right)^2 \qquad (7)\\ &= -\frac{1}{6}\left[(\partial_\mu\mathbf{n}\cdot\partial^\mu\mathbf{n})^3 - 3\left(\partial_\mu\mathbf{n}\cdot\partial^\mu\mathbf{n}\right)\left(\partial_\nu\mathbf{n}\cdot\partial_\rho\mathbf{n}\right)^2 + 2\left(\partial_\mu\mathbf{n}\cdot\partial^\nu\mathbf{n}\right)\left(\partial_\nu\mathbf{n}\cdot\partial^\rho\mathbf{n}\right)\left(\partial_\rho\mathbf{n}\cdot\partial^\mu\mathbf{n}\right)\right].\end{aligned}$$

The symmetry SO(4) ∼ SU(2) × SU(2) for $V = 0$ is thus manifest.

The target space (the vacuum manifold with $V = 0$) $\mathcal{M} \simeq \mathrm{SU}(2) \simeq S^3$ has a nontrivial homotopy group

$$\pi_3(M) = \mathbb{Z}, \tag{8}$$

which admits Skyrmions. The baryon number (the Skyrme charge) of $B \in \pi_3(S^3)$ is defined as

$$\begin{aligned} B &= -\frac{1}{24\pi^2}\int d^3x\, \epsilon^{ijk}\mathrm{tr}\,\left(U^\dagger\partial_i U U^\dagger\partial_j U U^\dagger\partial_k U\right)\\ &= \frac{1}{24\pi^2}\int d^3x\, \epsilon^{ijk}\mathrm{tr}\,\left(U^\dagger\partial_i U\partial_j U^\dagger\partial_k U\right)\\ &= -\frac{1}{12\pi^2}\int d^3x\, \epsilon^{ABCD}\epsilon^{ijk}\partial_i n_A\partial_j n_B\partial_k n_C n_D\\ &= -\frac{1}{2\pi^2}\int d^3x\, \epsilon^{ABCD}\partial_1 n_A\partial_2 n_B\partial_3 n_C n_D. \end{aligned} \tag{9}$$

Instead of the conventional potential term, we consider here the following potential term

$$V = m^2 n_4^2. \tag{10}$$

We call this potential the Heisenberg type. The vacua of this potential is determined by $n_4 = 0$, and thus the vacuum manifold is a sphere

$$\mathcal{M} \simeq S^2, \tag{11}$$

parametrized by n_1, n_2, n_3 with a constraint $\sum_{a=1,2,3} n_a^2 = 1$. From the homotopy group

$$\pi_2(\mathcal{M}) \simeq \mathbb{Z}, \tag{12}$$

this model admits a monopole, viz. a global monopole.

In our previous papers [17, 19, 30–32], we considered instead the potential term $V = m^2(1 - n_4^2)$, i.e. a modified mass term. This admits two discrete vacua and a domain wall interpolating between them.

In this paper, the potential (10) differs seemingly only by the overall sign. The physics described by this potential is, however, vastly different. The boundary condition at spatial infinity is

$$n_4 = 0, \qquad \text{for} \quad r \to \infty, \tag{13}$$

which has the vacuum manifold (11). The vacuum state is thus any point on the two-sphere, given by $n_1^2 + n_2^2 + n_3^2 = 1$. The potential (10) breaks the symmetry $\tilde{G} = \mathrm{SU}(2)_{\mathrm{L}} \times \mathrm{SU}(2)_{\mathrm{R}}$ down to $\mathrm{SU}(2)_{L+R}$, *explicitly.* This SU(2) or O(3) symmetry is, however, spontaneously broken down to O(2). The spontaneous breaking O(3)/O(2) gives rise to 2 Nambu-Goldstone bosons which remain massless as well as 1 massive pion. Abusing notation a bit, we can say that there are 2 massless pions and 1 massive pion. The phase of QCD we are trying to mimic, is high-density QCD at sufficiently high density; above the critical density for the formation of half-Skyrmions [6] and below the chiral restoration density. The potential (10) is an effective potential that can model this phase in the sense that it allows for half Skyrmions. It may or may not be the complete potential describing real QCD at mentioned densities, but in this paper we will study the above presented Skyrme-like models in the presence of said potential.

III. FRACTIONAL SKYRMION MOLECULES

In this section we will calculate numerical solutions of fractional molecules in the $B = 1$ sector, which are bound states of two half baryons. The only free parameter is the mass m, i.e. the coefficient in front of the Heisenberg-type potential. We will carry out the study in both the 2+4 and the 2+6 models. Instead of varying the mass, we will keep the mass fixed and vary the parameters (c_2, c_4) and (c_2, c_6) for the 2+4 and the 2+6 models, respectively. This includes the possibility of having $c_2 = 0$ which is not possible in the rescaled system where only the mass is varied. The $c_2 = 0$ region of parameter space is especially interesting due to the BPS properties that are present in that limit, see [16] for the 2+6 model and [33] for a possibility in the 2+4 model (although this requires a particular potential).

As an Ansatz for the initial guess fed to the relaxation procedure, we will simply use the hedgehog Ansatz, suitable for the $B = 1$ sector

$$\mathbf{n} = (-\cos f(r), \hat{\mathbf{x}} \sin f(r)) \,, \tag{14}$$

where $\hat{\mathbf{x}}$ is the 3-dimensional spatial unit vector and $r^2 = x^2+y^2+z^2$ is the radial coordinate. The relaxation method will then deform the initial guess away from the spherical initial guess to the correct minimal-energy state of molecular shape (due to the Heisenberg-type potential). Note that we have chosen a particular value on the vacuum manifold, namely $n_1 = -1$, which of course by O(3) symmetry is equivalent to any other choice.

We are now ready to perform the numerical calculation and we use the finite difference method to discretize the fields $\mathbf{n}$, feed the initial guess to the relaxation algorithm and simply evolve a linear time operator until the numerical precision of the solution satisfies our criteria.

We consider first the 2+4 model, i.e. $c_2 \geq 0, c_4 > 0$ and $c_6 = 0$. In Fig. 1 is shown an array of molecule baryon charge density isosurfaces for various choices of the coefficients (c_2, c_4) for fixed mass $m = 4$. The coloring scheme used is based on the hue-saturation-lightness (HSL) parameters and the hue is given by the phase $\arg(\pi_2 + i\pi_3)$, the lightness is given by $|\pi_1|$ and $\vec{\pi} \equiv \vec{n}/|\vec{n}|$ is a normalized 3-vector. All the numerical calculations throughout the paper are carried out on an 81^3 cubic lattice using the relaxation method. We observe that the molecular shape is most pronounced when the coefficients are small (which is clear, because that corresponds to a large mass) and even more so when $c_2 \ll c_4$.

In Figs. 2 and 3 are shown cross sections at $z = 0$ of the baryon charge density and energy density, respectively. The numerically integrated baryon charge density, denoted by $B^{\text{numerical}}$ gives a handle on the precision of the numerical solution, see Tab. I. Note that the molecular shape is slightly more pronounced in the energy density than in the baryon

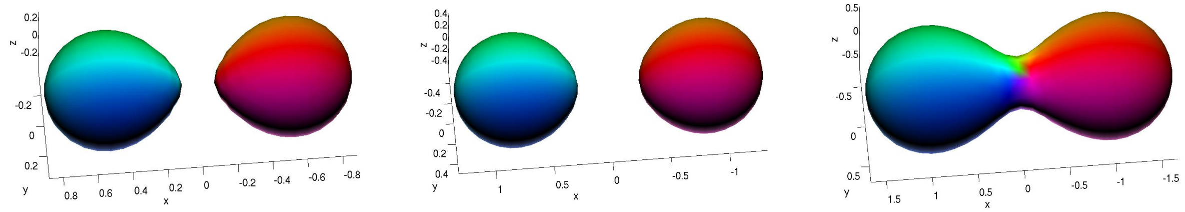

$c_2 = 0, c_4 = \frac{1}{4}$ $c_2 = 0, c_4 = 1$ $c_2 = 0, c_4 = 4$

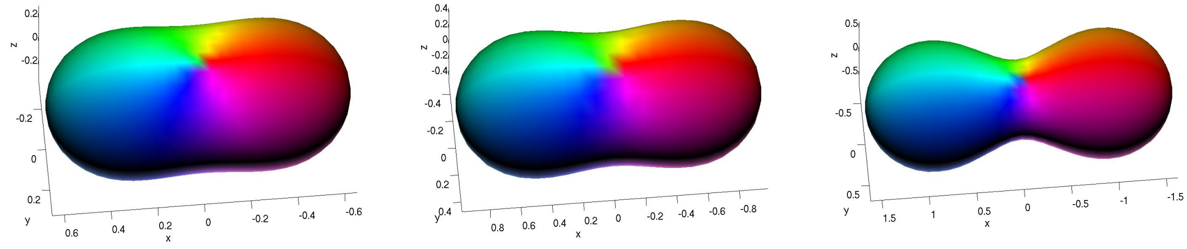

$c_2 = \frac{1}{4}, c_4 = \frac{1}{4}$ $c_2 = \frac{1}{4}, c_4 = 1$ $c_2 = \frac{1}{4}, c_4 = 4$

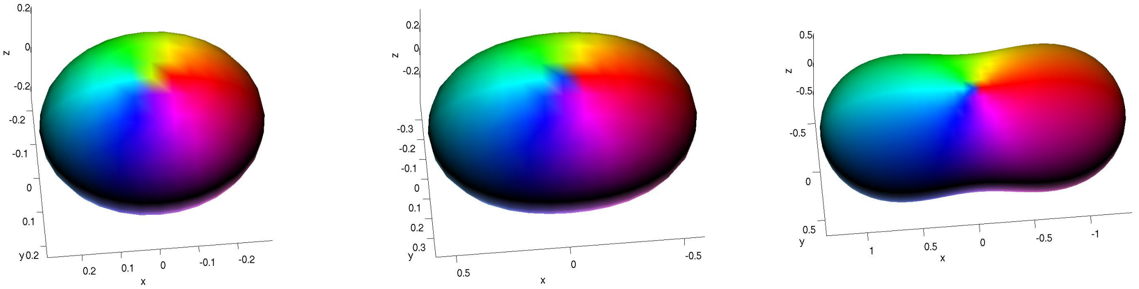

$c_2 = 1, c_4 = \frac{1}{4}$ $c_2 = 1, c_4 = 1$ $c_2 = 1, c_4 = 4$

FIG. 1: Isosurfaces showing the half-maximum of the baryon charge density in the 2+4 model for various choices of (c_2, c_4) for fixed mass $m = 4$. The color scheme represents the normalized 3-vector $\vec{\pi} = \frac{\vec{n}}{|\vec{n}|}$, where $\arg(\pi_2 + i\pi_3)$ is the hue and the lightness is given by $|\pi_1|$.

charge density, viz. the depth of the valley between the two peaks is deeper. In the cases $c_2 = 1, c_4 = \frac{1}{4}$ and $c_2 = c_4 = 1$, there is no valley between the two peaks; there is however still some amount of "polarization;" or better, there is a dipole moment. In order to quantify the amount to which the Skyrmion is moleculized, we define the following quantity

$$\mathfrak{p}^B \equiv 2\int d^3x\ \left(\mathrm{sign}(n_4)x\mathcal{B} - \mathrm{sign}(n_3)y\mathcal{B}\right), \tag{15}$$

which we call the baryonic dipole moment and

$$\mathcal{B} \equiv -\frac{1}{2\pi^2}\epsilon^{ABCD}\partial_1 n_A \partial_2 n_B \partial_3 n_C n_D, \tag{16}$$

is the baryon charge density. The physical meaning of $\mathfrak{p}^B$, which has units of length, is to which degree the baryon charge corresponding to the northern and southern hemisphere (distinguished by the sign of n_4) is separated compared to how the charge is distributed in the transverse direction. This quantity is absolute and should be compared to the size of the Skyrmion (see the figures). For a Skyrmion without the potential (10), the baryonic dipole moment vanishes: $\mathfrak{p}^B = 0$. For convenience we define the size of the Skyrmion as

$$\mathfrak{s}^B \equiv \sqrt{\int d^3x\ r^2\mathcal{B}}. \tag{17}$$

We mentioned already that the two coefficients c_2, c_4 are not independent of each other and they can be scaled to unity giving a mass which we will denote $m^{\text{canonical}}$ which can be calculated as

$$m^{\text{canonical}} = \frac{\sqrt{c_4}}{c_2}m, \tag{18}$$

where m is the mass in the noncanonically normalized Lagrangian, i.e. with $c_2 \neq 1$ and $c_4 \neq 1$. The values of $m^{\text{canonical}}$ for the various configurations shown in Figs. 1, 2 and 3 are given in Tab. I.

We will now consider the 2+6 model, i.e. $c_2 \geq 0, c_6 > 0$ and $c_4 = 0$. In Fig. 4 is shown an array of molecule baryon charge density isosurfaces for similar values of the coefficients (c_2, c_6) as in the previous case and for fixed mass $m = 4$. The coloring scheme is the same as used above. Again the molecular shape is mostly pronounced when the coefficients are small and $c_2 \ll c_6$. We also calculate the canonical mass,

$$m^{\text{canonical}} = \sqrt[4]{\frac{c_6}{c_2^3}}m, \tag{19}$$

i.e. the mass corresponding to a rescaled equation of motion with $c_2 = c_6 = 1$ and show those corresponding values in Tab. II.

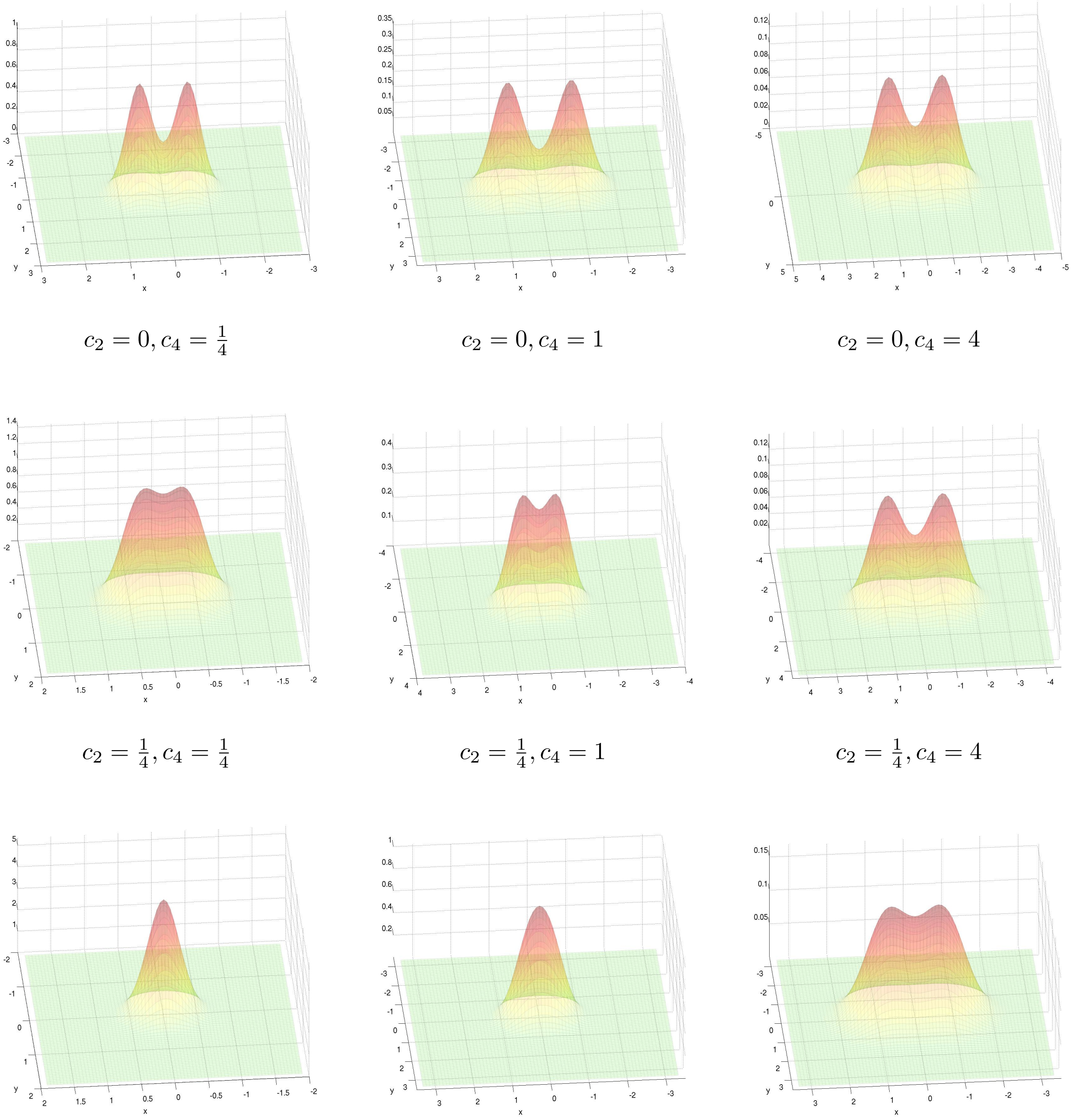

$c_2 = 0, c_4 = \frac{1}{4}$ $c_2 = 0, c_4 = 1$ $c_2 = 0, c_4 = 4$

$c_2 = \frac{1}{4}, c_4 = \frac{1}{4}$ $c_2 = \frac{1}{4}, c_4 = 1$ $c_2 = \frac{1}{4}, c_4 = 4$

$c_2 = 1, c_4 = \frac{1}{4}$ $c_2 = 1, c_4 = 1$ $c_2 = 1, c_4 = 4$

FIG. 2: Baryon charge density at a spatial slice through the molecule at $z = 0$ in the 2+4 model for various choices of (c_2, c_4) and for fixed mass $m = 4$.

In Figs. 5 and 6 are shown cross sections at $z = 0$ of the baryon charge density and energy density, respectively. The numerically integrated baryon charge density, denoted $B^{\text{numerical}}$ gives again a handle on the precision of the numerical solution, see Tab. II. We observe that the energy density is more spiky than the baryon charge density, hence more of a molecular

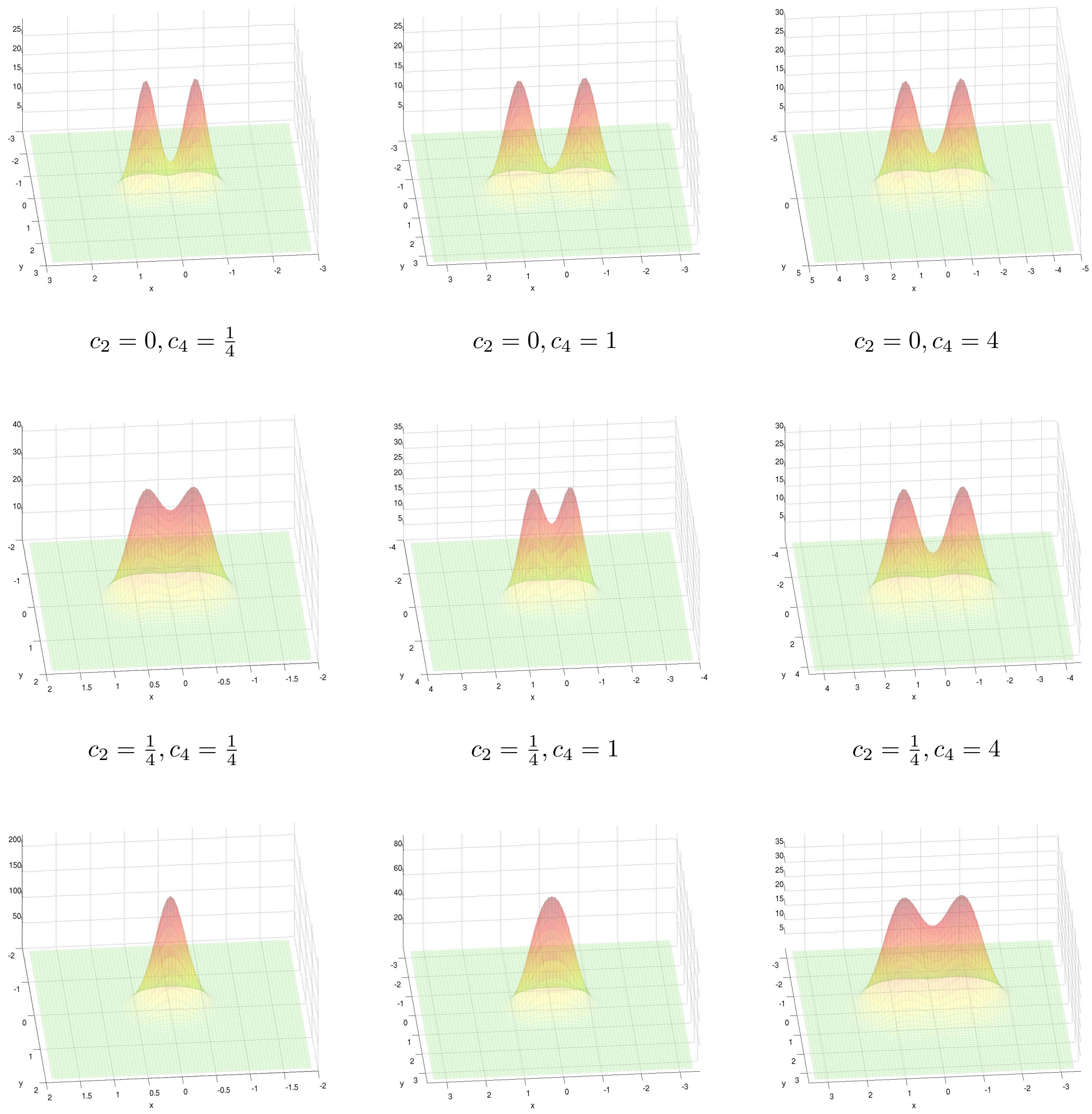

$c_2 = 0, c_4 = \frac{1}{4}$ $c_2 = 0, c_4 = 1$ $c_2 = 0, c_4 = 4$

$c_2 = \frac{1}{4}, c_4 = \frac{1}{4}$ $c_2 = \frac{1}{4}, c_4 = 1$ $c_2 = \frac{1}{4}, c_4 = 4$

$c_2 = 1, c_4 = \frac{1}{4}$ $c_2 = 1, c_4 = 1$ $c_2 = 1, c_4 = 4$

FIG. 3: Energy density at a spatial slice through the molecule at $z = 0$ in the 2+4 model for various choices of (c_2, c_4) and for fixed mass $m = 4$.

shape.

The case of $c_2 = 0$ and $c_6 > 0$ is particularly interesting because of its BPS and integrable properties. It is by now called the BPS Skyrme model [16]. The integrable property is very appealing since analytic solutions can readily be calculated for a large class of potentials.

TABLE I: The numerically integrated baryon charge, the numerically integrated energy and the numerically integrated baryonic dipole moment for the various configurations in the 2+4 model, shown in Figs. 1, 2 and 3.

c_2	c_4	$m^{\text{canonical}}$	$B^{\text{numerical}}$	$E^{\text{numerical}}$	$\mathfrak{p}^B$	$\mathfrak{s}^B$
0	$\frac{1}{4}$	∞	0.99969	18.930	0.575	0.772
0	1	∞	0.99986	52.720	0.970	1.151
0	4	∞	0.99989	154.74	0.998	1.472
$\frac{1}{4}$	$\frac{1}{4}$	2^3	0.99989	25.832	0.288	0.620
$\frac{1}{4}$	1	2^4	0.99967	65.527	0.478	0.901
$\frac{1}{4}$	4	2^5	0.99989	167.24	0.920	1.437
1	$\frac{1}{4}$	2^1	0.99962	40.078	0.087	0.426
1	1	2^2	0.99958	89.365	0.185	0.713
1	4	2^3	0.99972	203.93	0.635	1.282

TABLE II: The numerically integrated baryon charge, the numerically integrated energy and the numerically integrated baryonic dipole moment for the various configurations in the 2+6 model, shown in Figs. 4, 5 and 6.

c_2	c_6	$m^{\text{canonical}}$	$B^{\text{numerical}}$	$E^{\text{numerical}}$	$\mathfrak{p}^B$	$\mathfrak{s}^B$
$\frac{1}{4}$	$\frac{1}{4}$	2^3	0.99989	34.440	0.595	0.978
$\frac{1}{4}$	1	$2^{\frac{7}{2}}$	0.99986	61.728	0.863	1.278
$\frac{1}{4}$	4	2^4	0.99986	113.89	1.353	1.707
1	$\frac{1}{4}$	$2^{\frac{3}{2}}$	0.99986	60.705	0.281	0.822
1	1	2^2	0.99984	97.104	0.440	1.091
1	4	$2^{\frac{5}{2}}$	0.99985	161.15	0.708	1.442

Numerically, however, it is a rather difficult problem, because the Skyrmion in the BPS limit turns into a compacton [16], giving the soliton a finite size (hence no exponentially damped tail) and so a cusp in the fields at a finite distance. There is no cusp in the energy density, which is smooth, but the cusp in the fields requires a special technique in order to be studied numerically. We will not pursue this problem further in this paper.

The half-Skyrmion molecule has two components which we can interpret as global

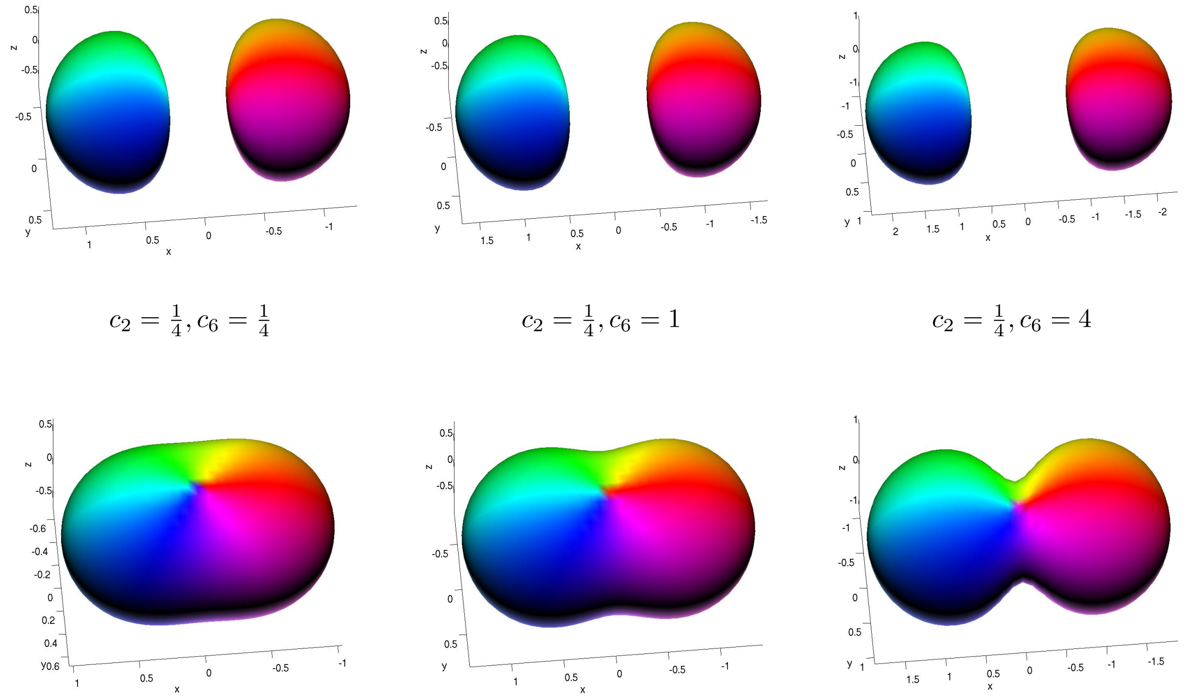

$c_2 = \frac{1}{4}, c_6 = \frac{1}{4}$ $c_2 = \frac{1}{4}, c_6 = 1$ $c_2 = \frac{1}{4}, c_6 = 4$

$c_2 = 1, c_6 = \frac{1}{4}$ $c_2 = 1, c_6 = 1$ $c_2 = 1, c_6 = 4$

FIG. 4: Isosurfaces showing the half-maximum of the baryon charge density in the 2+6 model for various choices of (c_2, c_6) for fixed mass $m = 4$. The color scheme is the same as that in Fig. 1.

monopoles, both of baryon charge 1/2. In Fig. 7 is shown a cross section at $z = 0$ of the n_4 component of the molecule in the 2+4 model with $c_2 = \frac{1}{4}$ and $c_4 = 1$, as an example. The same characteristic holds for all the molecules that we found in this section. The figure nicely shows that $n_4 = 0$, not only at infinity, but also on a plane separating the two constituents of the molecule (which is seen as a line in the cross section shown in Fig. 7). In the next section we will construct only one of the two constituents isolated, however, at the cost of having an infinite total energy of the configuration.

IV. FRACTIONAL SKYRMIONS AS GLOBAL MONOPOLES

In this section we will consider a limit in which one constituent of the molecule has been drawn away to infinity, thus leaving the molecule with only a half baryon number. The result is a half Skyrmion. This is usually not possible. The loop hole is that the configuration has

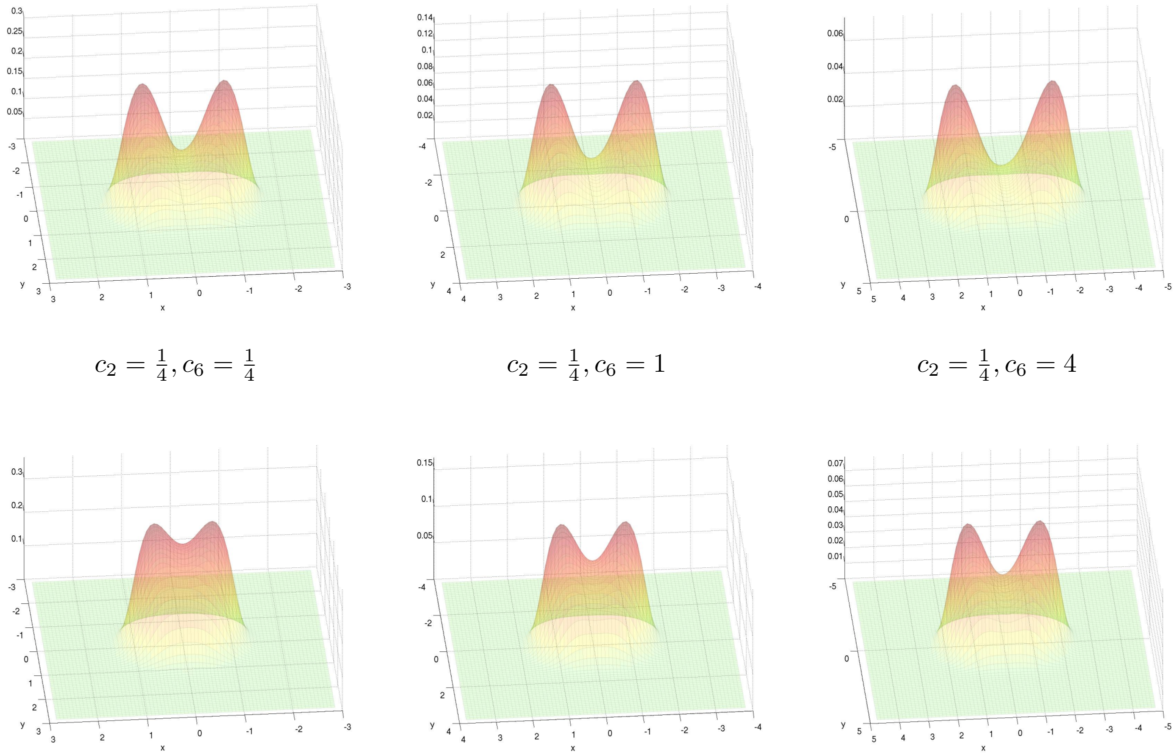

$c_2 = \frac{1}{4}, c_6 = \frac{1}{4}$ $c_2 = \frac{1}{4}, c_6 = 1$ $c_2 = \frac{1}{4}, c_6 = 4$

$c_2 = 1, c_6 = \frac{1}{4}$ $c_2 = 1, c_6 = 1$ $c_2 = 1, c_6 = 4$

FIG. 5: Baryon charge density at a spatial slice through the molecule at $z = 0$ in the 2+6 model for various choices of (c_2, c_6) and for fixed mass $m = 4$.

a divergent total energy. By inserting the Ansatz

$$\mathbf{n} = (\hat{\mathbf{x}} \sin f(r), \cos f(r)), \tag{20}$$

into the Lagrangian (5), we get

$$-\mathcal{L} = \frac{c_2}{2} f_r^2 + \frac{c_2}{r^2} \sin^2 f + \frac{c_4}{r^2} \sin^2(f) f_r^2 + \frac{c_4}{2r^4} \sin^4 f + \frac{c_6}{r^4} \sin^4(f) f_r^2 + \frac{m^2}{2} \cos^2 f, \tag{21}$$

which has the corresponding equation of motion

$$\begin{aligned} c_2 \left(f_{rr} + \frac{2}{r} f_r - \frac{1}{r^2} \sin 2f \right) + c_4 \left(\frac{2}{r^2} \sin^2(f) f_{rr} + \frac{1}{r^2} \sin(2f) f_r^2 - \frac{1}{r^4} \sin^2 f \sin 2f \right) \\ + c_6 \left(\frac{2}{r^4} \sin^4(f) f_{rr} - \frac{4}{r^5} \sin^4(f) f_r + \frac{2}{r^4} \sin^2 f \sin(2f) f_r^2 \right) + \frac{1}{2} m^2 \sin 2f = 0, \end{aligned} \tag{22}$$

where $f_r \equiv \partial_r f$. The difference between this Lagrangian with corresponding equation of motion and the normal case with a mass term is that the potential $\sin^2 f$ is replaced with

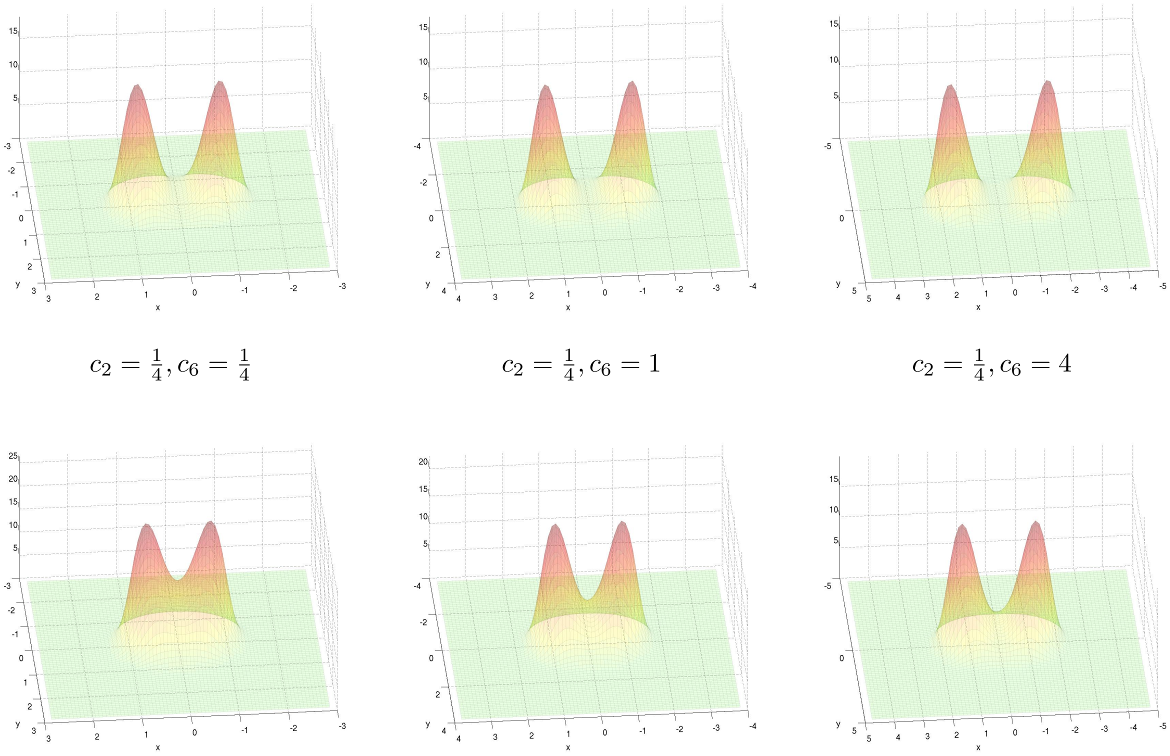

$c_2 = \frac{1}{4}, c_6 = \frac{1}{4}$ $c_2 = \frac{1}{4}, c_6 = 1$ $c_2 = \frac{1}{4}, c_6 = 4$

$c_2 = 1, c_6 = \frac{1}{4}$ $c_2 = 1, c_6 = 1$ $c_2 = 1, c_6 = 4$

FIG. 6: Energy density at a spatial slice through the molecule at $z = 0$ in the 2+6 model for various choices of (c_2, c_6) and for fixed mass $m = 4$.

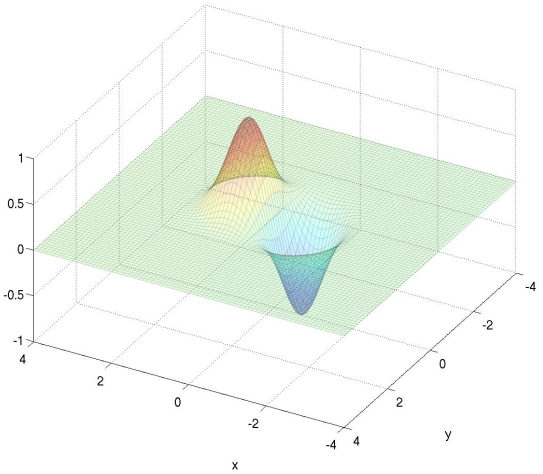

FIG. 7: The n_4 component at a spatial slice through a molecule at $z = 0$ in the 2+4 model with $c_2 = \frac{1}{4}$ and $c_4 = 1$.

$\cos^2 f$ and in turn $-\sin 2f$ in the equation of motion becomes $+\sin 2f$. We therefore need to consider the boundary conditions for this system in order to construct a half Skyrmion. One possibility is to choose

$$\text{southern molecule constituent:} \qquad f(0) = \pi, \qquad f(\infty) = \frac{\pi}{2}, \tag{23}$$

giving a half Skyrmion winding on only the southern hemisphere of the target space. Alternatively, we could have chosen

$$\text{northern molecule constituent:} \qquad f(0) = 0, \qquad f(\infty) = \frac{\pi}{2}, \tag{24}$$

giving instead a half anti-Skyrmion which winds only on the northern hemisphere of the target space.

In Figs. 8 and 9 are shown numerical solutions for the half Skyrmion winding on only the southern hemisphere of the target space (i.e. $n_4 \in [-1, 0]$) for the 2+4 and 2+6 model, respectively. The half Skyrmion can live in isolation only at the cost of an infinite total energy. Figs. 8c and 9c show that the energy density multiplied by r^2, i.e. $4\pi r^2 \mathcal{E}$ goes to a constant and hence the total energy picks up a linear divergence in the radial integral $E \propto R_{\rm max}$, where $R_{\rm max}$ is the radial cut off of the integral. All the baryon charge densities integrate numerically to one half.

V. HIGHER BARYON NUMBERS

In this section we make a first attempt to make solutions with higher baryon numbers, i.e. $B > 1$. As we *ab initio* do not know the shape of the global minimizers, we use the relaxation method with different initial guesses. The two guesses we choose here are the axially symmetric Ansatz

$$\mathbf{n} = \left(-\cos f(r), \sin\theta \sin B\phi \sin f(r), \sin\theta\cos B\phi \sin f(r), \cos\theta \sin f(r)\right), \tag{25}$$

and the following Ansatz using a rational map R:

$$\mathbf{n} = \left(-\cos f(r), \frac{R+\bar{R}}{1+R\bar{R}} \sin f(r), \frac{i(\bar{R}-R)}{1+R\bar{R}} \sin f(r), \frac{1-R\bar{R}}{1+R\bar{R}} \sin f(r)\right), \tag{26}$$

with the symmetries found to minimize the Skyrmions without the potential (10). For the appropriate rational maps, R, see Refs. [20, 21]. Note again that we have chosen a particular

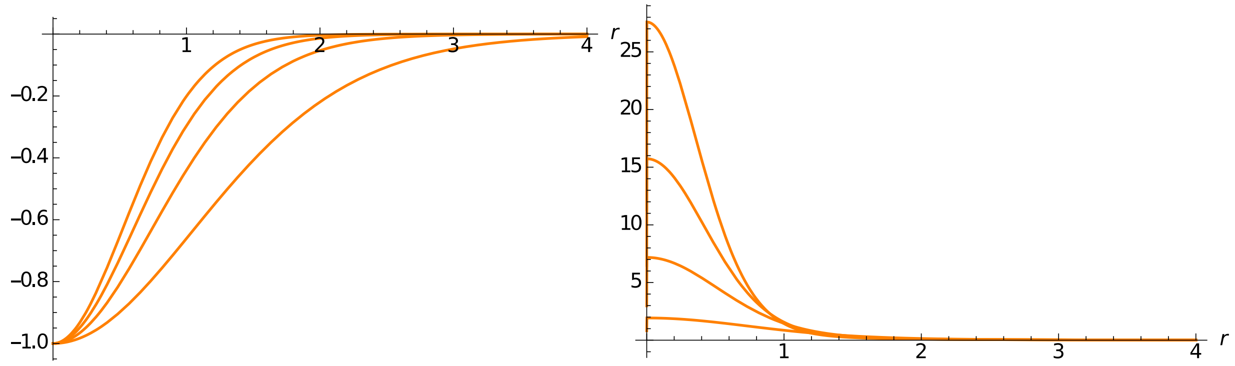

(a) $n_4 = \cos f$

(b) $\mathcal{E}$

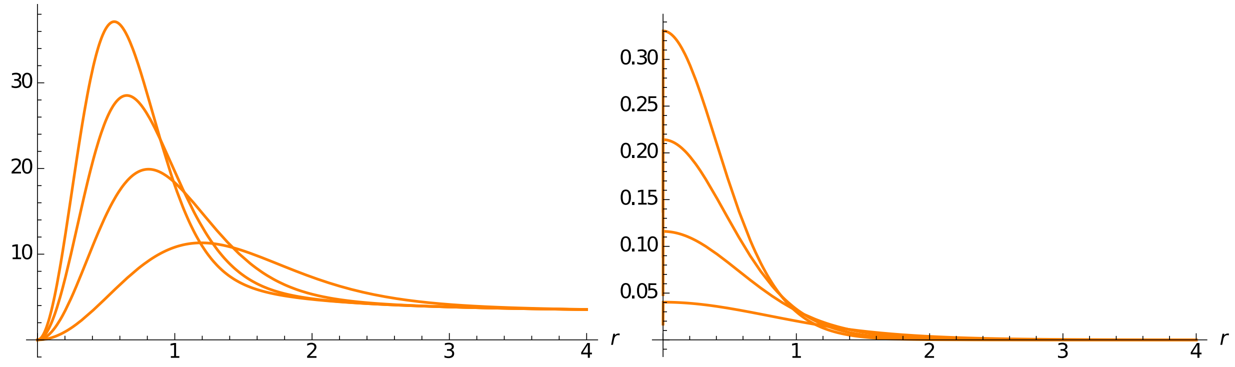

(c) $4\pi r^2\mathcal{E}$

(d) $\mathcal{B}$

FIG. 8: An isolated half Skyrmion (a global monopole) in the 2+4 model for various masses m: (a) the radial field profile $n_4 = \cos f$. (b) and (c) the energy density $\mathcal{E}$ and $4\pi r^2\mathcal{E}$, respectively. The latter shows the divergence in the total energy. (d) is the baryon charge density. The chosen parameters are $c_2 = \frac{1}{4}$, $c_4 = 1$ and $m = 1, 2, 3, 4$.

value on the vacuum manifold, i.e. $n_1 = -1$ which by O(3) symmetry is equivalent to any other choice.

We begin with the 2+4 model and calculate the numerical solutions for the first six baryon numbers, i.e. $B = 2, 3, 4, 5, 6$ ($B = 1$ was already made in Sec. III). For concreteness, we fix the parameters $c_2 = \frac{1}{4}$, $c_4 = 1$ and $m = 4$, corresponding to a canonical mass $m^{\rm canonical} = 16$. We find that the lowest-energy states take the shapes of rings (beads on rings) and show the numerical solutions as isosurfaces at the half-maximum baryon charge densities in Fig. 10. These solutions are made with the axially-symmetric initial guess (25). We again use the numerically integrated baryon charge density, $B^{\rm numerical}$ as a handle on the precision of the numerical solution, see Tab. III. In this table we also show the total energy

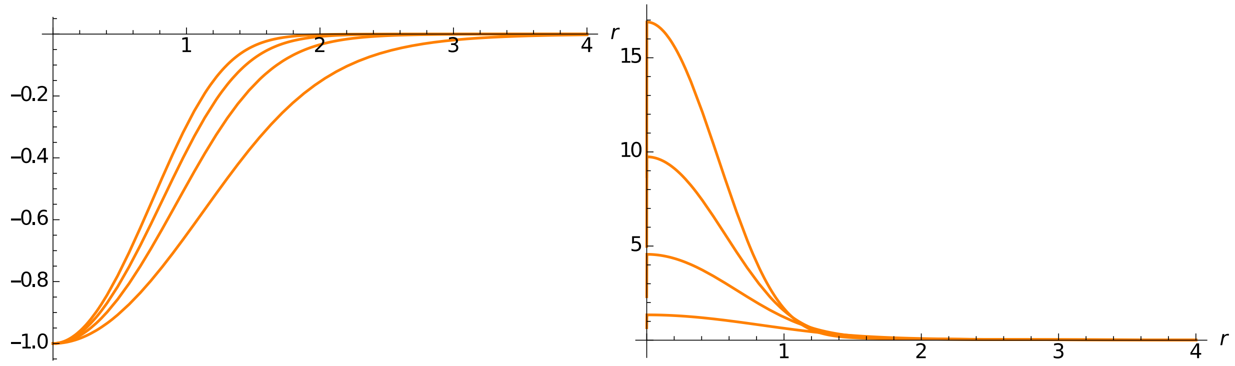

(a) $n_4 = \cos f$

(b) $\mathcal{E}$

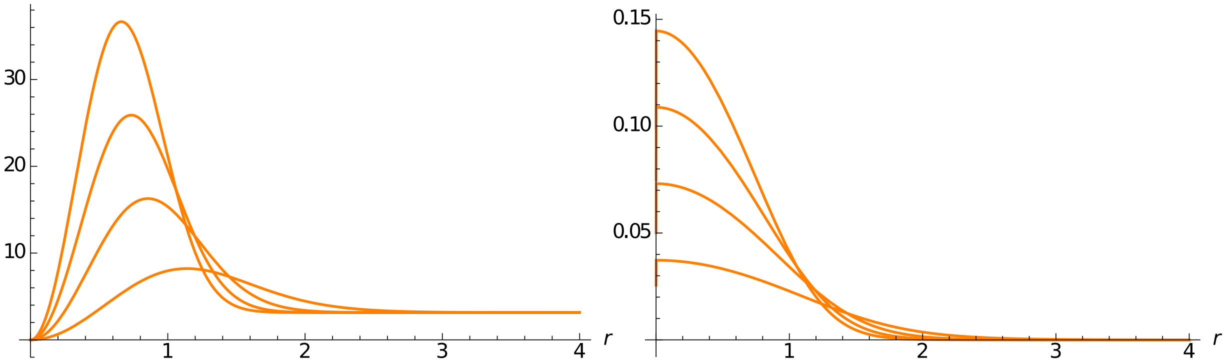

(c) $4\pi r^2 \mathcal{E}$

(d) $\mathcal{B}$

FIG. 9: An isolated half Skyrmion (a global monopole) in the 2+6 model for various masses m: (a) the radial field profile $n_4 = \cos f$. (b) and (c) the energy density $\mathcal{E}$ and $4\pi r^2 \mathcal{E}$, respectively. The latter shows the divergence in the total energy. (d) is the baryon charge density. The chosen parameters are $c_2 = \frac{1}{4}$, $c_6 = 1$ and $m = 1, 2, 3, 4$.

per unit baryon charge, $E^{\rm numerical}/B$, which tells us whether the higher-charged solution is stable or only metastable. We find that all the higher-charged solutions we have calculated, namely $B = 2, 3, 4, 5, 6$ are in fact stable (at least among this type of configurations).

The isosurface shows the three-dimensional structure of the solution, but not the profile shape of the baryon-charge density or energy density. Therefore, as before, we show cross sections at $z = 0$ of the baryon charge density and energy density in Fig. 11 and 12, respectively. Note that again the molecular shape is slightly more pronounced in the energy density than in the baryon charge density, viz. the depth of the valleys between the peaks are deeper. Finally, we notice that the molecular shape (by which we mean that half a unit of baryon charge is spatially localized) is far more pronounced for higher baryon charges

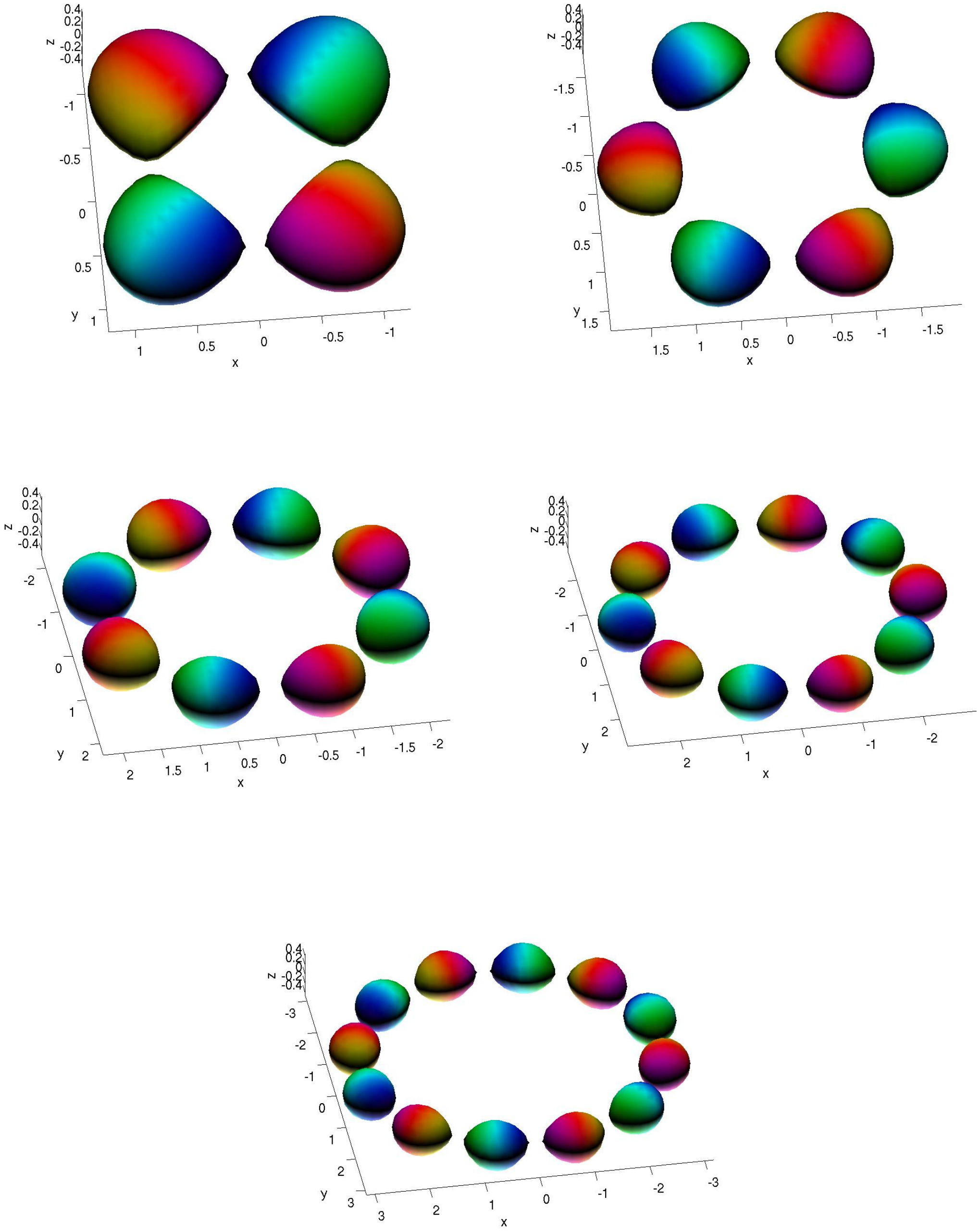

FIG. 10: Isosurfaces showing the half-maximum of the baryon charge density in the 2+4 model for baryon numbers $B = 2, 3, 4, 5, 6$ with $c_2 = \frac{1}{4}$, $c_4 = 1$ and fixed mass $m = 4$. The color scheme is the same as that in Fig. 1.

$B > 1$ than for $B = 1$, for the same coefficients, i.e. $c_2 = \frac{1}{4}$, $c_4 = 1$ and $m = 4$.

TABLE III: The numerically integrated baryon charge and energy per unit baryon charge for higher baryon numbers in the 2+4 model.

B	$B^{\rm numerical}$	$E^{\rm numerical}/B$
1	0.99967	65.52(7)
2	1.9994	61.5(3)
3	2.9979	61.0(6)
4	3.9971	60.8(9)
5	4.9964	60.7(9)
6	5.9957	60.5(5)

As we mentioned already, we do not *ab initio* know the symmetries or spatial structure of the *global* energy-minimizing solutions. Therefore we have tried also different initial conditions to check whether we can obtain lower-energy solutions with the same baryon numbers compared to those obtained with the axially-symmetric initial guess (25). Explicitly, we have tried the rational-map Ansatz with the rational maps that minimize the energy without the potential (10). We found these solutions to have higher energies than those shown here (or being spatially disconnected) and more details are given in Appendix A.

We will now consider the 2+6 model and calculate numerical solutions for the first five baryon numbers, i.e. $B = 2, 3, 4, 5$ ($B = 1$ was made in Sec. III). For concreteness, we fix here the parameters $c_2 = \frac{1}{4}$, $c_6 = 1$ and $m = 4$, corresponding to a canonical mass $m^{\rm canonical} = 8\sqrt{2}$. As in the case of the 2+4 model, we find again that the lowest-energy states take the shapes of rings (beads on rings). These solutions are made with the axially-symmetric initial guess (25). In Fig. 13 are shown the isosurfaces of the baryon charge densities at their respective half-maximum values of the numerical solutions. The numerically integrated baryon charge and total energy per unit baryon charge are displayed in Tab. IV. We find as in the case of the 2+4 model, that all the calculated solutions with higher-baryon numbers, $B > 1$, are stable (as opposed to metastable) among this type of configurations.

The cross sections at $z = 0$ of the baryon charge densities and energy densities are shown in Fig. 14 and 15, respectively. Note that again the molecular shape is slightly more pronounced in the energy density than in the baryon charge density, viz. the depth of the valleys between the peaks are deeper. In fact, the slices of the energy densities suggest that

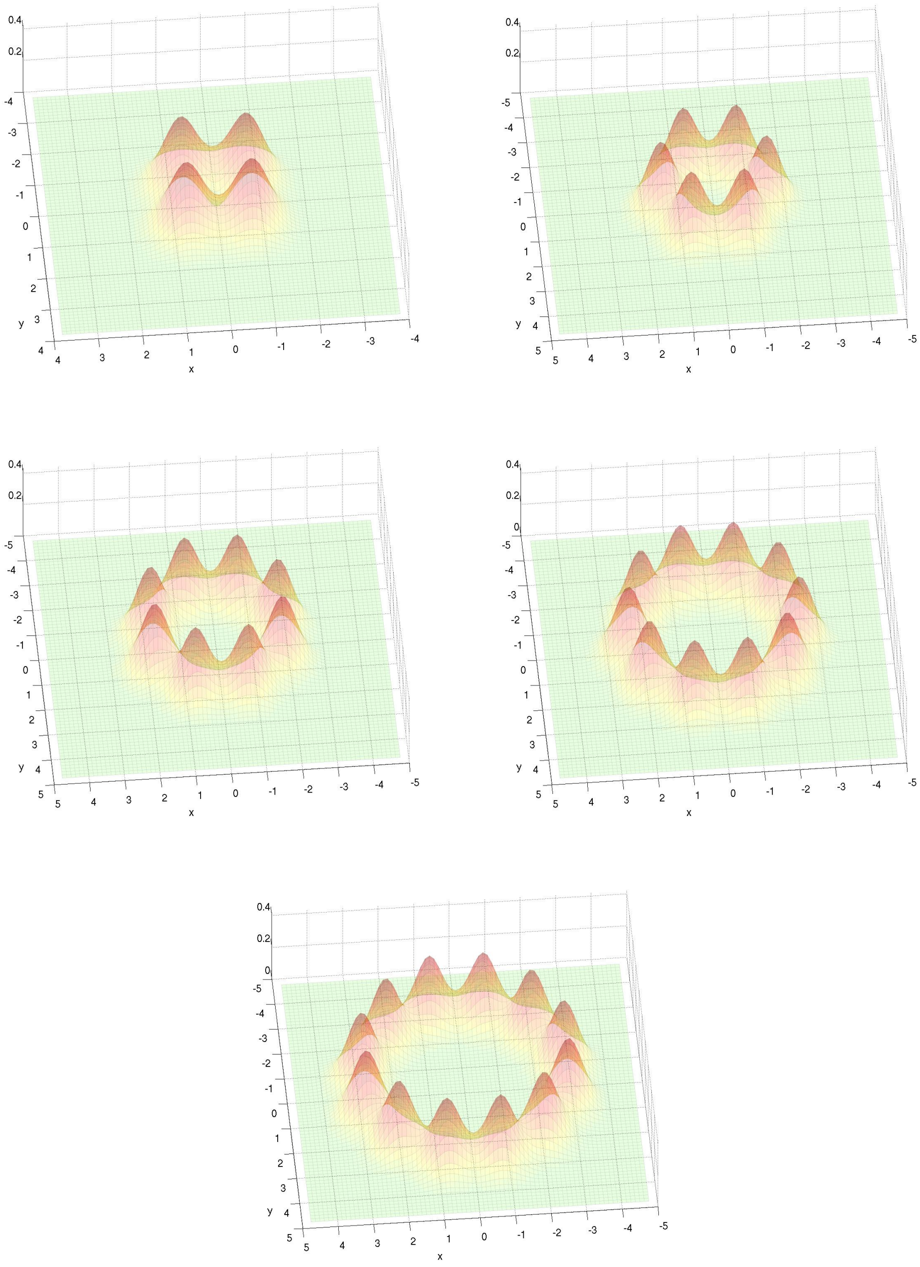

FIG. 11: Baryon charge density at a spatial slice through the $B = 2, 3, 4, 5, 6$ molecules at $z = 0$ in the 2+4 model for various choices of (c_2, c_4) and for fixed mass $m = 4$.

the beads are not spatially connected. This is, however, not true. From the slices of baryon charge densities, we see that the beads are connected and from Tab. IV, we can see that there is in fact a small binding energy. Asymptotically, however, for $B \to \infty$ the binding

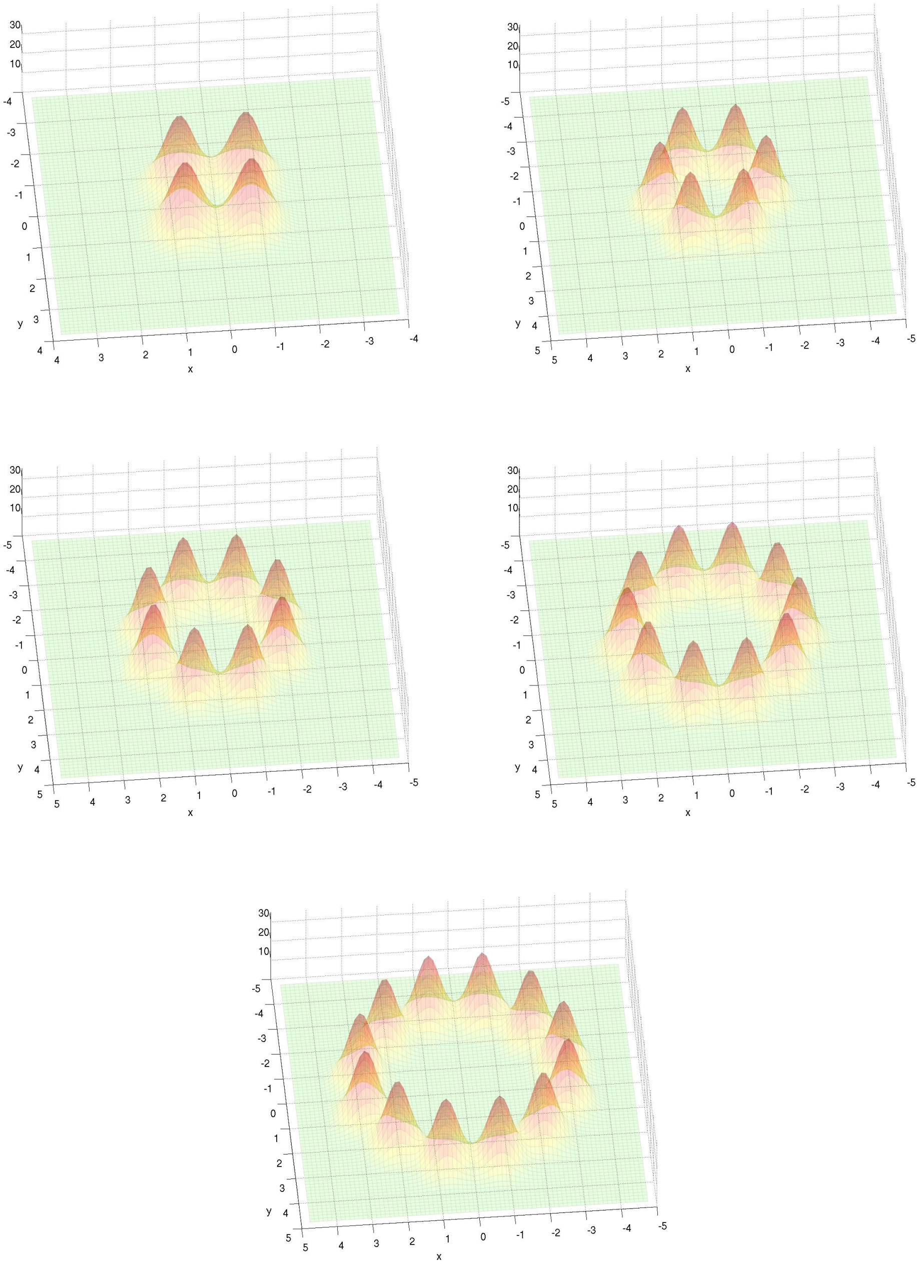

FIG. 12: Energy density at a spatial slice through the $B = 2, 3, 4, 5, 6$ molecules at $z = 0$ in the 2+4 model for various choices of (c_2, c_4) and for fixed mass $m = 4$.

energy may go to zero (in the 2+6 model for the given parameters).

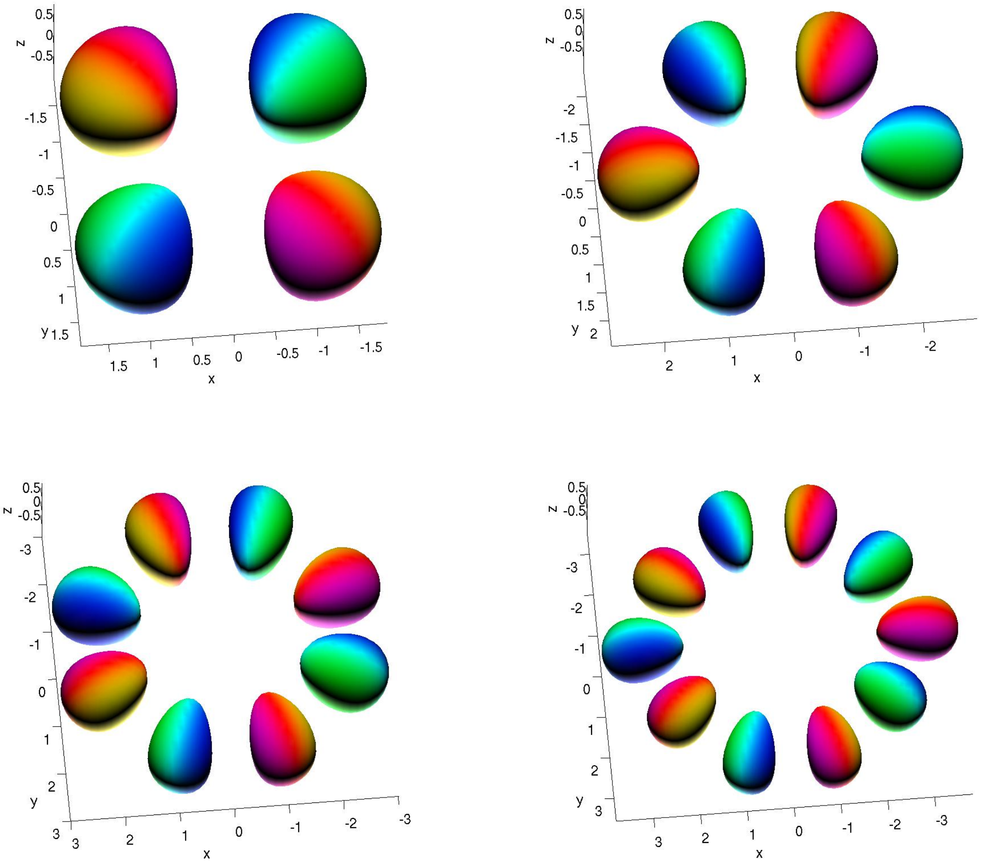

FIG. 13: Isosurfaces showing the half-maximum of the baryon charge density in the 2+6 model for baryon numbers $B = 2, 3, 4, 5$ with $c_2 = \frac{1}{4}$, $c_6 = 1$ and fixed mass $m = 4$. The color scheme is the same as that in Fig. 1.

VI. MOLECULES WITH UNEQUAL FRACTIONS

In this section, we show that by a modification of the potential (10), we can create a molecule, still with two components, but with unevenly distributed baryon charge. The modified potential is

$$V = \frac{1}{2} m^2 (n_4 - c)^2, \tag{27}$$

giving rise to a molecule with two components with localized baryon charge $(1 + c)/2$ and $(1 - c)/2$, respectively. This potential thus requires different asymptotic boundary conditions and hence different initial guesses. Since we consider only the $B = 1$ sector here, a modified

TABLE IV: The numerically integrated baryon charge and energy per unit baryon charge for higher baryon numbers in the 2+6 model.

B	$B^{\text{numerical}}$	$E^{\text{numerical}}/B$
1	0.99986	61.72(8)
2	1.9998	59.2(7)
3	2.9990	59.1(6)
4	3.9985	59.0(7)
5	4.9981	58.9(1)

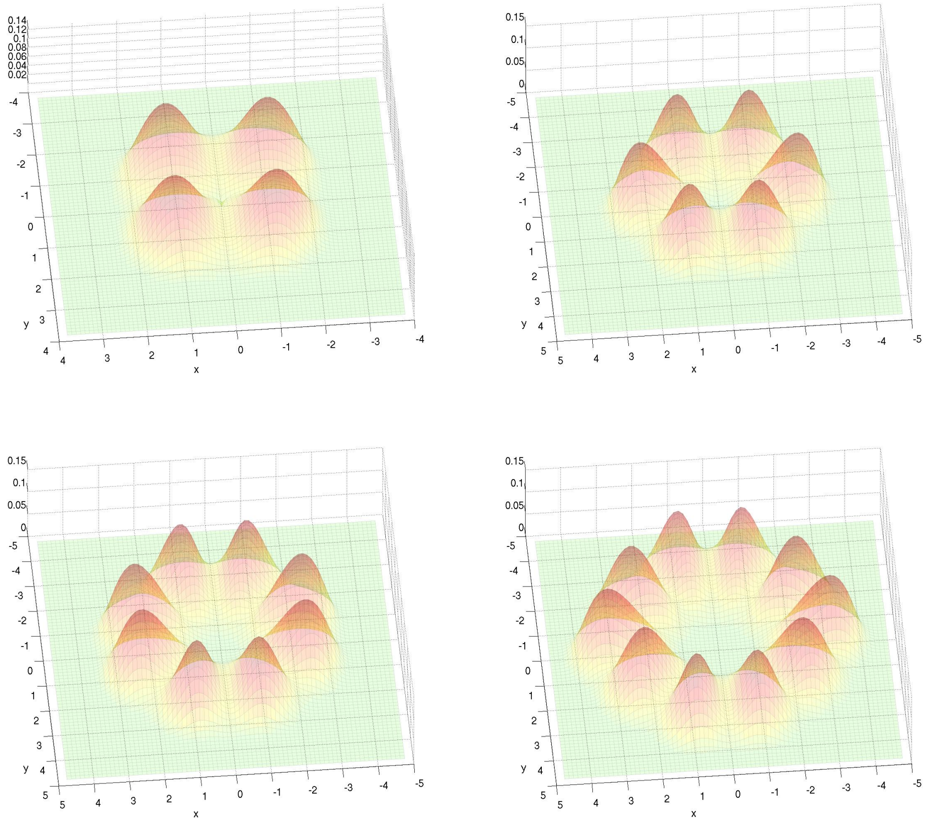

FIG. 14: Baryon charge density at a spatial slice through the $B = 2, 3, 4, 5$ molecules at $z = 0$ in the 2+6 model for various choices of (c_2, c_6) and for fixed mass $m = 4$.

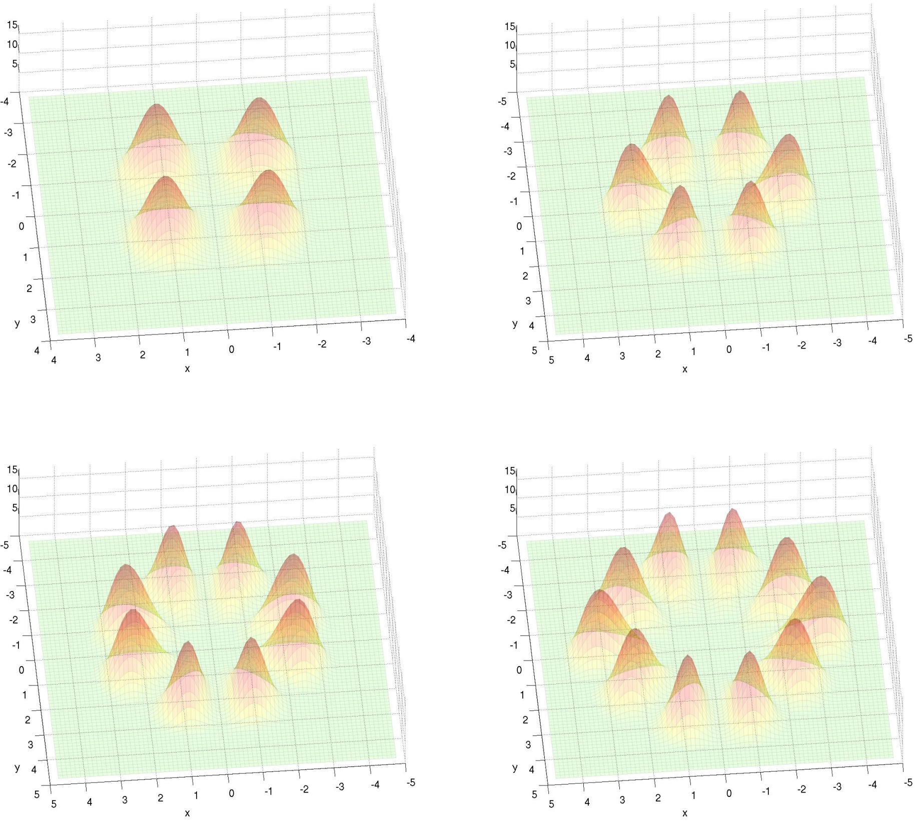

FIG. 15: Energy density at a spatial slice through the $B = 2, 3, 4, 5$ molecules at $z = 0$ in the 2+6 model for various choices of (c_2, c_6) and for fixed mass $m = 4$.

hedgehog Ansatz is sufficient

$$\mathbf{n} = \Big(c\,\hat{x}\sin f(r) - \sqrt{1-c^2}\cos f(r), \hat{y}\sin f(r), \hat{z}\sin f(r), c\cos f(r) + \sqrt{1-c^2}\hat{x}\sin f(r)\Big)\,, \tag{28}$$

which satisfies the vacuum equation at $r \to \infty$ provided $f(\infty) = 0$.

In the following we will choose a concrete example, setting $c = \frac{1}{3}$, which is interesting, because the two components of the baryon should contain $\frac{2}{3}$ and $\frac{1}{3}$ of the unit baryon charge, respectively. For concreteness, we will keep the parameters that we have used in Sec. V, namely: $c_2 = \frac{1}{4}$, $c_4 = 1$ ($c_6 = 1$) and $m = 4$ in the case of the 2+4 (2+6) model. The numerical solutions are shown in Figs. 16 and 17.

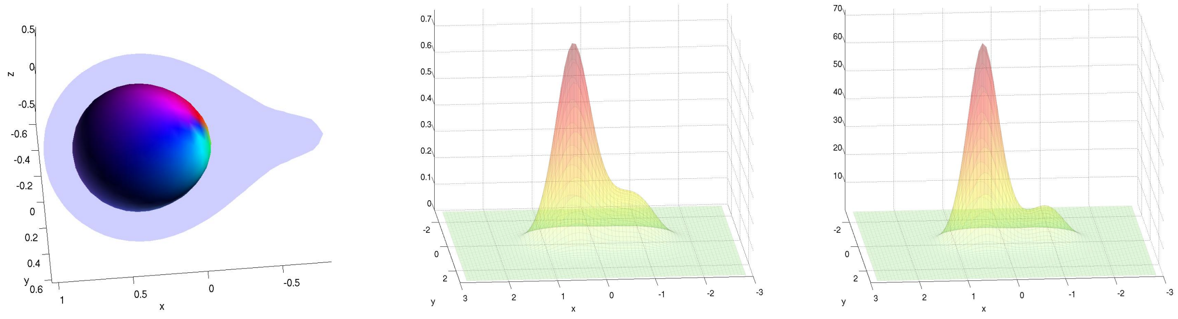

(a) isosurface (b) baryon charge density (c) energy density

FIG. 16: Unequal fractional molecule with $c = \frac{1}{3}$ giving a molecule in the 2+4 model with two components of charge $\frac{2}{3}$ and $\frac{1}{3}$, respectively. (a) shows the isosurface of the baryon charge density at half-maximum value and there is an added shadow which is an isosurface at one quarter of the maximum value. (b) and (c) show xy-slices (at $z = 0$) of the baryon charge density and the energy density, respectively. The parameters are $c_2 = \frac{1}{4}$, $c_4 = 1$ and $m = 4$. The color scheme is the same as that in Fig. 1. The numerically integrated baryon charge is $B^{\text{numerical}} = 0.99974$.

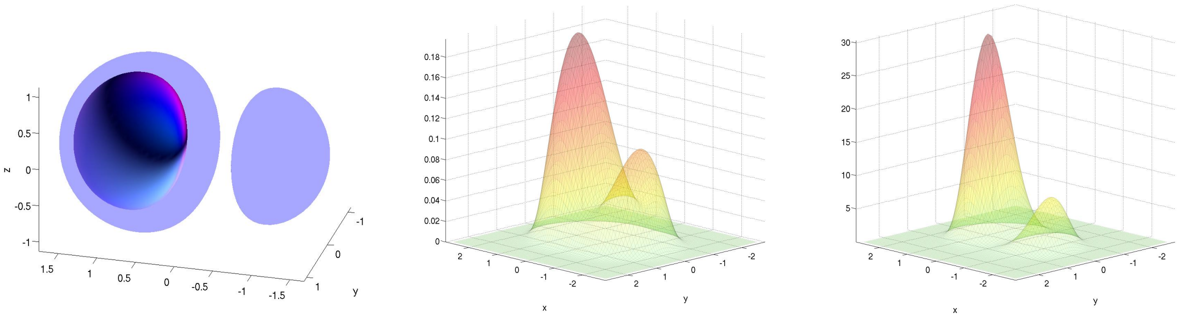

(a) isosurface (b) baryon charge density (c) energy density

FIG. 17: Unequal fractional molecule with $c = \frac{1}{3}$ giving a molecule in the 2+6 model with two components of charge $\frac{2}{3}$ and $\frac{1}{3}$, respectively. (a) shows the isosurface of the baryon charge density at half-maximum value and there is an added shadow which is an isosurface at one quarter of the maximum value. (b) and (c) show xy-slices (at $z = 0$) of the baryon charge density and the energy density, respectively. The parameters are $c_2 = \frac{1}{4}$, $c_6 = 1$ and $m = 4$. The color scheme is the same as that in Fig. 1. The numerically integrated baryon charge is $B^{\text{numerical}} = 0.99995$.

VII. SUMMARY AND DISCUSSION

We have constructed fractional Skyrmions and their molecules in the Skyrme model with the potential term, $V = m^2 n_4^2$. As for higher-derivative terms, we have considered the conventional fourth-order derivative term, viz. the Skyrme term or the sixth-order derivative term being the baryon number current squared. One molecule consists of a pair of a global monopole and anti-monopole, each with half a baryon number. Since an isolated global monopole has divergent energy in an infinite space, the constituents are confined. We have also constructed an isolated fractional Skyrmion as a global monopole (which thus has a divergent total energy). We have then constructed Skyrmion solutions with higher baryon numbers up to $B = 6$, and have found that configurations in the form of beads on rings are energetically stable. We have also found other metastable configurations for $B = 3$ and $B = 5$, but exhausting all possible metastable configurations remains as a future problem. Finally by considering the potential term $V \sim m^2(n_4 - c)^2$, we have found that fractional Skyrmions have baryon numbers that are not equal to one half. As an example, we have constructed a molecule with fractional Skyrmions with the baryon numbers $1/3 + 2/3$.

We have shown that our choice of the potential (10) as an effective low-energy potential is able to describe the half-Skyrmion phase which should be present in QCD at high density [6]. In Ref. [6], which studies a holographic model, quite different from our low-energy effective field theory model, the ω and ρ mesons were needed to consistently describe the high density phase where the half Skyrmions exist. Whether our simple model with our choice of effective potential is able to capture the relevant phenomenological features of QCD at high density is a very interesting and important question that is left as a future work.

As a lower dimensional analog, there exists a fractional baby-Skyrmion molecule consisting of a pair of a global vortex and anti-vortex with half π_2 charges in the O(3) model with the XY (or easy-plane) potential term $V = m^2 n_3^2$ in $d = 2 + 1$ dimensions. In this model too, baby Skyrmions as beads on a ring were found as (meta)stable configurations [10, 11]. However, the lowest-energy configurations of higher topological numbers are of the form of square lattices of fractional lumps [9]. We expect a cubic lattice of fractional Skyrmions for higher baryon numbers in our 3+1 dimensional case.

If we add a potential $V_2 = m_2^2 n_1$ with $m_2 < m$ in the O(3) model with the XY-potential term $V = m^2 n_3^2$ in $d = 2 + 1$ dimensions, vortices are connected by a sine-Gordon soliton.

Therefore, fractional lumps are linearly confined by the sine-Gordon soliton. This happens in fact in two-gap (or two-component) superconductors described by a Landau-Ginzburg Lagrangian in the form of a U(1) gauge theory with two charged scalar fields ϕ_1 and ϕ_2. The two fields are coupled through the Josephson term $L_{\rm J} = \gamma\phi_1^*\phi_2$ in the case of two-gap superconductors, but not for two-component superconductors. In either case, it admits a molecule of half-quantized vortices [34]. In the presence of the Josephson term, fractional vortices are connected [35] by a sine-Gordon kink [36]. In the strong gauge-coupling limit, the model reduces to an O(3) sigma model with the potential term $V = m^2 n_3^2$ complemented by $V_2 = \gamma n_1$ induced by the Josephson term [37, 38], and the molecule reduces to a fractional baby-Skyrmion molecule mentioned above [39]. In the same way, if we add a potential that breaks the SO(3) symmetry, possessed by the vacuum, such as $V_2 = m_2^2 n_1$ $(m_2 < m)$, fractional Skyrmions constituting a molecule will be connected by a baby-Skyrmion string, realizing linear confinement of fractional Skyrmions.

The Bogomol'nyi-Prasad-Sommerfield (BPS) Skyrme model, proposed recently [16], consists of only the sixth-order derivative term as well as appropriate potentials. This model admits exact solutions with compact support. By choosing the potential in this paper, we may be able to construct exact solutions of a fractional Skyrmion molecule.

Fractional Skyrmions in the O(4) model (or the Skyrme model) on $\mathbb{R}^2 \times S^1$ were discussed in Ref. [40], in which our potential term is related to the boundary condition where the field n_4 changes the sign along S^1. A rather different origin of fractional topological charge was also found for vortices and lumps [41]. A unified understanding of fractional topological charges will be an important future work.

Acknowledgments

The work of M. N. is supported in part by Grant-in-Aid for Scientific Research No. 25400268 and by the "Topological Quantum Phenomena" Grant-in-Aid for Scientific Research on Innovative Areas (No. 25103720) from the Ministry of Education, Culture, Sports, Science and Technology (MEXT) of Japan. S. B. G. thanks Keio University for hospitality during which this project took shape. S. B. G. thanks the Recruitment Program of High-end Foreign Experts for support.

Appendix A: Rational map Ansatz in the 2+4 model

In this section we investigate numerical solutions with different initial guesses to be used by the relaxation method, in particular, we consider the rational-map Ansatz (26) with an appropriate rational map R. For $B = 1$ and $B = 2$, the axially symmetric Ansatz (25) is a very educated guess due to the high level of symmetry. For $B = 3$ and higher B, without the potential (10), the lowest-energy state turns out to have a discrete symmetry instead of axial symmetry [20, 21]. As already mentioned, we do not *a priori* know what symmetry or shapes the minimizer of the energy may have, and therefore we try the minimizers which are found to be the lowest-energy states without the potential (10) as initial guess also here, i.e. with the potential (10). For concreteness, we use the 2+4 model with $c_2 = \frac{1}{4}$, $c_4 = 1$ and $m = 4$ and calculate numerical solutions for $B = 3, 4, 5$. The isosurfaces of the baryon charge density at half-maximum values are shown in Fig. 18.

The first case, $B = 3$, found using the rational map with a tetrahedral symmetry turns out to give a numerical solution which is only metastable, see Tab. V for a comparison of the energies of the numerical solutions. In order to demonstrate that the two clusters of three half units of Skyrme charge are really connected, we display a cross section of the baryon charge density and energy density at $x = 0$ in Fig. 19. Of course, no half unit of Skyrme charge can be spatially localized (without a tail) and thus neither can three half units. Both the baryon charge density and the energy density on the yz slices in Fig. 19 have maximum values around one quarter of their respective global maximum values (i.e. in the three-dimensional space).

The case, $B = 4$, found using the rational map with a cubic symmetry gave rise to a solution that split up into two $B = 2$ axially symmetric solutions; i.e. they are both chargewise and energetically separated. Due to the $B = 2$ solution with axial symmetry having a larger energy per unit baryon charge than the $B = 4$ solution, see Tab. III, two $B = 2$ solutions thus have a higher energy than the $B = 4$ solution being a ring (with beads).

The last case, i.e. $B = 5$ is like the $B = 3$ case spatially connected, but is made with a rational map having an octahedral symmetry. It is however energetically only metastable, viz. it has a higher energy than the solution made using the axially symmetric Ansatz.

The bottom line is that the lowest-energy solutions for the molecules are all found using

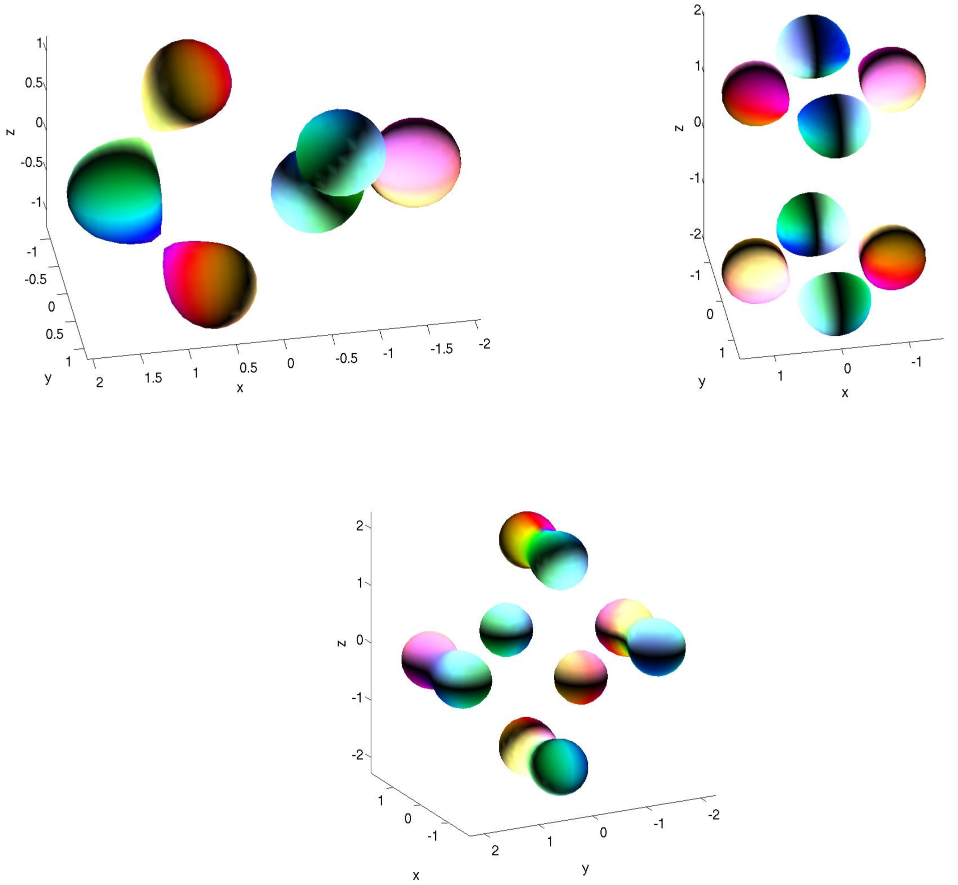

FIG. 18: Isosurfaces showing the half-maximum of the baryon charge density in the 2+4 model for baryon numbers $B = 3, 4, 5$ with $c_2 = \frac{1}{4}$, $c_4 = 1$ and fixed mass $m = 4$. These numerical solutions have been obtained using the rational-map Ansatz (26) as initial guesses. The color scheme is the same as that in Fig. 1.

the axially symmetric Ansatz (25). Using the rational-map Ansatz (26), we have found metastable solutions for the $B = 3, 5$ cases, which however are energetically prone to decay.

Appendix B: Low-mass limit of the 2+4 model

For completeness, we provide a series of numerical solutions for the 2+4 model, for the, in this paper, most studied case; i.e. $c_2 = \frac{1}{4}$, $c_4 = 1$ with various masses $m = 0, \frac{1}{2}, 1, \frac{3}{2}, 2, \frac{5}{2}, 3, \frac{7}{2}$ whereas the case of $m = 4$ is used throughout the paper. The isosurfaces of the baryon

TABLE V: A comparison of the numerically integrated baryon charge and energy per unit baryon charge for higher baryon numbers in the 2+4 model for different initial guesses. The * denotes a solution that is spatially disconnected.

B (initial guess)	$B^{\text{numerical}}$	$E^{\text{numerical}}/B$
3 (axially symmetric)	2.9979	61.0(6)
3 (tetrahedral)	2.9986	61.1(7)
4 (axially symmetric)	3.9971	60.8(9)
$4^\star$ (cubic)	3.9971	61.5(2)
5 (axial)	4.9964	60.7(9)
5 (octahedral)	4.9964	61.5(4)

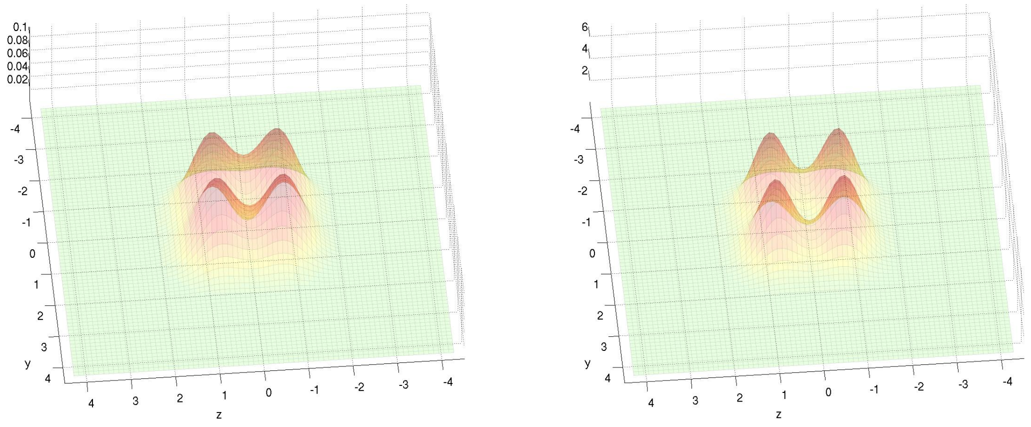

baryon charge density

energy density

FIG. 19: Cross sections at $x = 0$ showing the baryon charge density and energy density in the 2+4 model for baryon numbers $B = 3$ with $c_2 = \frac{1}{4}$, $c_4 = 1$ and fixed mass $m = 4$. This numerical solution has been obtained using the rational-map Ansatz (26) as an initial guess.

charge densities of the solutions are shown in Fig. 20. The baryon charges, masses, dipole moments and sizes are given in Tab. VI.

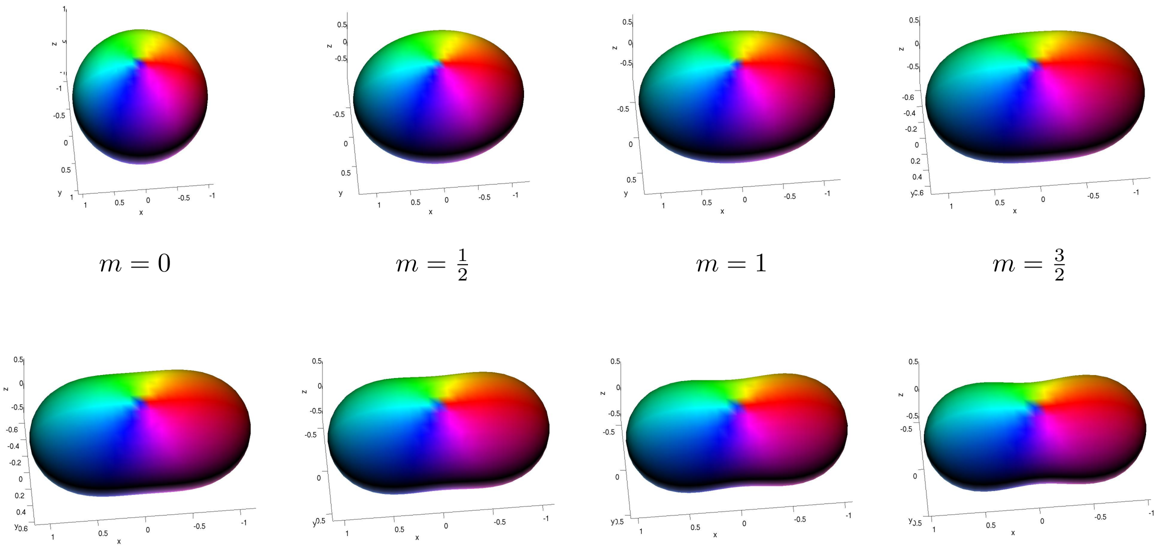

$m = 0$ $m = \frac{1}{2}$ $m = 1$ $m = \frac{3}{2}$

$m = 2$ $m = \frac{5}{2}$ $m = 3$ $m = \frac{7}{2}$

FIG. 20: Isosurfaces showing the half-maximum of the baryon charge density in the 2+4 model for a single baryon with masses $m = 0, \frac{1}{2}, 1, \frac{3}{2}, 2, \frac{5}{2}, 3, \frac{7}{2}$ and the usual fixed coefficients $c_2 = \frac{1}{4}$, $c_4 = 1$. The color scheme is the same as that in Fig. 1.

TABLE VI: The numerically integrated baryon charge, the numerically integrated energy and the numerically integrated baryonic dipole moment for the various masses shown in Fig. 20.

m	$B^{\text{numerical}}$	$E^{\text{numerical}}$	$\mathfrak{p}^B$	$\mathfrak{s}^B$
0	0.9963	35.731	0	1.876
$\frac{1}{2}$	0.9895	38.044	0.334	1.763
1	0.9997	43.930	0.364	1.441
$\frac{3}{2}$	0.9999	48.457	0.398	1.271
2	0.9999	52.446	0.419	1.157
$\frac{5}{2}$	0.9998	56.069	0.432	1.072
3	0.9998	59.421	0.439	1.005
$\frac{7}{2}$	0.9997	62.556	0.443	0.950
4	0.9997	65.527	0.478	0.901

[1] T. H. R. Skyrme, "A Unified Field Theory of Mesons and Baryons," Nucl. Phys. **31**, 556 (1962); "A Nonlinear field theory," Proc. Roy. Soc. Lond. A **260**, 127 (1961).

[2] G. S. Adkins, C. R. Nappi and E. Witten, "Static Properties of Nucleons in the Skyrme Model," Nucl. Phys. B **228**, 552 (1983).

[3] E. Witten, "Global Aspects of Current Algebra," Nucl. Phys. B **223**, 422 (1983); "Current Algebra, Baryons, and Quark Confinement," Nucl. Phys. B **223**, 433 (1983).

[4] T. Sakai and S. Sugimoto, "Low energy hadron physics in holographic QCD," Prog. Theor. Phys. **113**, 843 (2005) [hep-th/0412141]; "More on a holographic dual of QCD," Prog. Theor. Phys. **114**, 1083 (2005) [hep-th/0507073].

[5] H. Hata, T. Sakai, S. Sugimoto and S. Yamato, "Baryons from instantons in holographic QCD," Prog. Theor. Phys. **117**, 1157 (2007) [hep-th/0701280 [hep-th]].

[6] Y. L. Ma, M. Harada, H. K. Lee, Y. Oh, B. Y. Park and M. Rho, "Dense baryonic matter in the hidden local symmetry approach: Half-skyrmions and nucleon mass," Phys. Rev. D **88**, no. 1, 014016 (2013) [arXiv:1304.5638 [hep-ph]]; "Dense baryonic matter in conformally-compensated hidden local symmetry: Vector manifestation and chiral symmetry restoration," Phys. Rev. D **90**, 034015 (2014) [arXiv:1308.6476 [hep-ph]]; Y. L. Ma, M. Harada, H. K. Lee, Y. Oh and M. Rho, "Skyrmions, half-skyrmions and nucleon mass in dense baryonic matter," Int. J. Mod. Phys. Conf. Ser. **29**, 1460238 (2014) [arXiv:1312.2290 [hep-ph]].

[7] B. M. A. Piette, B. J. Schroers and W. J. Zakrzewski, "Multi - Solitons In A Two-Dimensional Skyrme Model," Z. Phys. C **65**, 165 (1995) [arXiv:hep-th/9406160]; "Dynamics of baby skyrmions," Nucl. Phys. B **439**, 205 (1995) [arXiv:hep-ph/9410256].

[8] T. Weidig, "The baby Skyrme models and their multi-skyrmions," Nonlinearity **12**, 1489-1503 (1999) [arXiv:hep-th/9811238].

[9] J. Jaykka and M. Speight, "Easy plane baby skyrmions," Phys. Rev. D **82**, 125030 (2010) [arXiv:1010.2217 [hep-th]].

[10] M. Kobayashi and M. Nitta, "Fractional vortex molecules and vortex polygons in a baby Skyrme model," Phys. Rev. D **87**, no. 12, 125013 (2013) [arXiv:1307.0242 [hep-th]].

[11] M. Kobayashi and M. Nitta, "Vortex polygons and their stabilities in Bose-Einstein condensates and field theory," J. Low. Temp. Phys. **175**, 208 (2014) [arXiv:1307.1345 [cond-

mat.quant-gas]].

[12] B. J. Schroers, “Bogomolny solitons in a gauged O(3) sigma model,” Phys. Lett. B **356**, 291 (1995) [hep-th/9506004]; “The Spectrum of Bogomol’nyi solitons in gauged linear sigma models,” Nucl. Phys. B **475**, 440 (1996) [hep-th/9603101].

[13] J. M. Baptista, “Vortex equations in Abelian gauged sigma-models,” Commun. Math. Phys. **261**, 161 (2006) [math/0411517 [math-dg]].

[14] M. Nitta and W. Vinci, “Decomposing Instantons in Two Dimensions,” J. Phys. A **45**, 175401 (2012) [arXiv:1108.5742 [hep-th]].

[15] A. Alonso-Izquierdo, W. G. Fuertes and J. M. Guilarte, “Two Species of Vortices in a massive Gauged Non-linear Sigma Model,” arXiv:1409.8419 [hep-th].

[16] C. Adam, J. Sanchez-Guillen and A. Wereszczynski, “A Skyrme-type proposal for baryonic matter,” Phys. Lett. B **691**, 105 (2010) [arXiv:1001.4544 [hep-th]]; “A BPS Skyrme model and baryons at large N_c,” Phys. Rev. D **82**, 085015 (2010) [arXiv:1007.1567 [hep-th]].

[17] S. B. Gudnason and M. Nitta, “Baryonic sphere: a spherical domain wall carrying baryon number,” Phys. Rev. D **89**, 025012 (2014) [arXiv:1311.4454 [hep-th]].

[18] S. B. Gudnason and M. Nitta, “Effective field theories on solitons of generic shapes,” arXiv:1407.2822 [hep-th].

[19] S. B. Gudnason and M. Nitta, “Baryonic Torii: Toroidal baryons in a generalized Skyrme model,” Phys. Rev. D **91**, 045027 (2015) [arXiv:1410.8407 [hep-th]].

[20] R. A. Battye and P. M. Sutcliffe, “Symmetric skyrmions,” Phys. Rev. Lett. **79**, 363 (1997) [hep-th/9702089].

[21] C. J. Houghton, N. S. Manton and P. M. Sutcliffe, “Rational maps, monopoles and Skyrmions,” Nucl. Phys. B **510**, 507 (1998) [hep-th/9705151].

[22] Y. Brihaye and D. H. Tchrakian, “Solitons/instantons in d-dimensional gauged Skyrme models,” Nonlinearity **11**, 891 (1998) [hep-th/9805059].

[23] Y. Brihaye, B. Kleihaus and D. H. Tchrakian, “Dyon - Skyrmion lumps,” J. Math. Phys. **40**, 1136 (1999) [hep-th/9805059].

[24] B. Kleihaus, D. H. Tchrakian and F. Zimmerschied, “Monopole skyrmions,” J. Math. Phys. **41**, 816 (2000) [hep-th/9907035].

[25] Y. Brihaye, B. Hartmann and D. H. Tchrakian, “Monopoles and dyons in SO(3) gauged Skyrme models,” J. Math. Phys. **42**, 3270 (2001) [hep-th/0010152].

[26] Y. Brihaye, J. Burzlaff, V. Paturyan and D. H. Tchrakian, “Comment on the soliton of the SO(3) gauged Skyrme model,” Nonlinearity **15**, 385 (2002) [hep-th/0109034].

[27] D. Y. Grigoriev, P. M. Sutcliffe and D. H. Tchrakian, “Skyrmed monopoles,” Phys. Lett. B **540**, 146 (2002) [hep-th/0206160].

[28] Y. Brihaye, C. T. Hill and C. K. Zachos, “Bounding gauged skyrmion masses,” Phys. Rev. D **70**, 111502 (2004) [hep-th/0409222].

[29] Y. Brihaye, J. Burzlaff and D. H. Tchrakian, “Asymptotic analysis of the Skyrmed monopole,” Phys. Rev. D **77**, 107701 (2008) [arXiv:0712.0549 [hep-th]].

[30] M. Nitta, “Correspondence between Skyrmions in 2+1 and 3+1 Dimensions,” Phys. Rev. D **87**, 025013 (2013) [arXiv:1210.2233 [hep-th]]; “Matryoshka Skyrmions,” Nucl. Phys. B **872**, 62 (2013) [arXiv:1211.4916 [hep-th]].

[31] S. B. Gudnason and M. Nitta, “Domain wall Skyrmions,” Phys. Rev. D **89**, 085022 (2014) [arXiv:1403.1245 [hep-th]].

[32] S. B. Gudnason and M. Nitta, “Incarnations of Skyrmions,” Phys. Rev. D **90**, 085007 (2014) [arXiv:1407.7210 [hep-th]].

[33] D. Harland, “Topological energy bounds for the Skyrme and Faddeev models with massive pions,” Phys. Lett. B **728**, 518 (2014) [arXiv:1311.2403 [hep-th]].

[34] E. Babaev, “Vortices with Fractional Flux in Two-Gap Superconductors and in Extended Faddeev Model,” Phys. Rev. Lett. **89** (2002) 067001; E. Babaev, A. Sudbo and N. W. Ashcroft, “A superconductor to superfluid phase transition in liquid metallic hydrogen,” Nature **431**, 666 (2004); J. Smiseth, E. Smorgrav, E. Babaev and A. Sudbo, “Field- and temperature induced topological phase transitions in the three-dimensional N-component London superconductor,” Phys. Rev. B **71**, 214509 (2005) [arXiv:cond-mat/0411761]; E. Babaev and N. W. Ashcroft, “Violation of the London law and Onsager-Feynman quantization in multicomponent superconductors,” Nature Phys. **3**, 530 (2007).

[35] J. Goryo, S. Soma and H. Matsukawa, “Deconfinement of vortices with continuously variable fractions of the unit flux quanta in two-gap superconductors,” Euro Phys. Lett. **80**, 17002 (2007) [arXiv:cond-mat/0608015].

[36] Y. Tanaka, “Phase instability in multi-band superconductors,” J. Phys. Soc. Jp. **70**, 2844 (2001); “Soliton in Two-Band Superconductor,” Phys. Rev. Lett. **88**, 017002 (2001).

[37] M. Nitta, “Josephson vortices and the Atiyah-Manton construction,” Phys. Rev. D **86**, 125004

(2012) [arXiv:1207.6958 [hep-th]].

[38] M. Kobayashi and M. Nitta, "Sine-Gordon kinks on a domain wall ring," Phys. Rev. D **87**, 085003 (2013) [arXiv:1302.0989 [hep-th]].

[39] K. Kasamatsu, M. Tsubota and M. Ueda, "Vortex Molecules in Coherently Coupled Two-Component Bose-Einstein Condensates," Phys. Rev. Lett **93**, 250406 (2004); "Vortices in multicomponent Bose-Einstein condensates," Int. J. Mod. Phys. **B** 19, 1835 (2005); M. Cipriani and M. Nitta, "Crossover between integer and fractional vortex lattices in coherently coupled two-component Bose-Einstein condensates," Phys. Rev. Lett. **111**, 170401 (2013) [arXiv:1303.2592 [cond-mat.quant-gas]]; M. Nitta, M. Eto and M. Cipriani, "Vortex molecules in Bose-Einstein condensates," J. Low. Temp. Phys. **175**, 177 (2013) [arXiv:1307.4312 [cond-mat.quant-gas]].

[40] M. Nitta, "Fractional instantons and bions in the O (N) model with twisted boundary conditions," JHEP **1503**, 108 (2015) [arXiv:1412.7681 [hep-th]].

[41] M. Eto, T. Fujimori, S. B. Gudnason, K. Konishi, T. Nagashima, M. Nitta, K. Ohashi and W. Vinci, "Fractional Vortices and Lumps," Phys. Rev. D **80**, 045018 (2009) [arXiv:0905.3540 [hep-th]].